Electronic Supplementary Information (ESI)

Water - Stable 2-D Zr MOFs with Exceptional UO_2^{2+} Sorption Capability

Nikos Panagiotou[a], Ioanna Liatsou[a], Anastasia Pournara[b], Giasemi K. Angeli[c], Rafaela Maria Giappa[c], Emmanuel Tylianakis[c], Manolis J. Manos[b], George E. Froudakis[c], Pantelis N. Trikalitis[c], Ioannis Pashalidis[a], Anastasios J. Tasiopoulos*[,a]

[a.] *Department of Chemistry, University of Cyprus, 1678 Nicosia, Cyprus Fax: ++357-22-895451; Tel: ++357-22-892765; E-mail: atasio@ucy.ac.cy*

[b.] *Department of Chemistry, University of Ioannina, 45110 Ioannina, Greece*

[a.] *Department of Chemistry, University of Crete, Voutes 71003, Heraklion, Greece*

Table of Contents

Experimental Section

Reagent grade chemicals were obtained from commercial sources (Aldrich, Merck, Alfa Aesar, TCI, etc.) and used without further purification. All synthetic procedures were carried out in air.

UCY-13: Solid $ZrCl_4$ (0.116 g, 0.498 mmol) was added in one portion to a clear solution of $H_2HFPBBA$ ($H_2HFPBBA$ = 4,4'-(Hexafluoroisopropylidene)bis(benzoic acid)) (0.294 g, 0.75 mmol) in DMF (10 ml) and HCOOH (4.8 ml, 5.86 g, 127 mmol) in a 23 ml glass vial and sonicated until complete dissolution of the reactants. The vial was sealed, placed in an oven at 130 ^oC and left undisturbed for ~72 h. Then it was cooled to room temperature and X-ray quality colorless rhombic plate crystals of **UCY-13** were isolated by filtration, washed with DMF (3 x15 ml) and acetone (5 x15 ml) and dried in air. Yield ~ 65% based on $ZrCl_4$. Elemental analysis calcd for **UCY-13**·8DMF·16HCOOH ($Zr_6F_{24}O_{72}N_8C_{108}H_{136}$): C 35.04; H 3.70; N 3.03; found: C 35.38; H 3.57; N 2.93.

UCY-14: Solid $ZrCl_4$ (0.264 g, 1.13 mmol) was added in one portion to a pale yellow suspension of H_2OBA (H_2OBA = 4,4'-Oxybis(benzoic acid)) (0.372g, 1.44 mmol) in DMF (5 ml) and HCOOH (1.2 ml, 1.46 g, 31.8 mmol) in a 23 ml glass vial and sonicated until complete dissolution of the reactants. The vial was sealed, placed in an oven at 130^oC and left undisturbed for ~72h. Then it was cooled to room temperature and X-ray quality colorless rhombic plate crystals of **UCY-14** were isolated by filtration, washed with DMF (3 x 15 ml) and acetone (5 x 15 ml) and dried in air. Yield ~ 70% based on $ZrCl_4$. Elemental analysis calcd for **UCY-14**·6DMF·6HCOOH ($Zr_6O_{54}N_6C_{81}H_{100}$): C 37.87; H 3.92; N 3.27; found: C 37.64; H 3.74; N 3.55.

Stability tests. Stability in organic solvents was investigated as follows: in 5 ml of the corresponding organic solvent were suspended 50 mg of as synthesized MOF and the mixture was stirred for ~24 hours while the solvent was replenished every 8 hours. The powder was then isolated and analyzed by pxrd and TGA. Stability in aqueous solutions was investigated following the below procedure: In 5 ml aqueous solutions of the target pH value (adjusted with the addition of a strong acid (HCl) or base (NaOH)) or an inorganic salt was added the as synthesized MOF (50 mg) of and the suspension was stirred for 24 hours. The powder was then isolated by filtration and analyzed by pxrd. Simulated seawater was prepared according to a previous report.[1]

Physical measurements.

Elemental analyses (C, H, O) were performed by the in-house facilities of the University of Cyprus, Chemistry Department. IR spectra were recorded on ATR in the 4000 − 700 cm^{-1} range using a Shimadzu Prestige − 21 spectrometer. Pxrd diffraction patterns were recorded on a Shimazdu 6000 Series X-ray diffractometer (Cu Kα radiation, λ = 1.5418 Å). Variable temperature diffractograms were carried out in the 25 ^{o}C- 450 ^{o}C range with 25 ^{o}C min^{-1} increase rate. Samples remained for 5 minutes at the corresponding temperature before measurement. Thermal stability studies were performed with a Shimadzu TGA 50 thermogravimetric analyzer. ^{1}H and ^{19}F-NMR spectra were recorded on a Bruker Avance III 300 MHz spectrometer at 25 ^{o}C. Chemical shift values in ^{1}H NMR spectra were reported in parts per million (ppm) relative to tetramethylsilane. Digestion of the samples was achieved with 0.5M KOH in D_2O.

Single crystal X-ray crystallography. Single Crystal X-ray diffraction data were collected on a Rigaku Supernova A diffractometer, equipped with a CCD area detector utilizing Cu-Kα (λ = 1.5418 Å) radiation. A suitable crystal was mounted on a Hampton cryoloop with Paratone-N oil and transferred to a goniostat where it was cooled for data collection. The structures were solved by direct methods using SHELXT and refined on F^2 using full-matrix least squares using SHELXL14.1.[2] Software packages used: CrysAlis CCD for data collection, CrysAlis RED for cell refinement and data reduction[3], WINGX for geometric calculations[4], and DIAMOND for molecular graphics[5]. The non-H atoms were treated anisotropically, whereas the aromatic hydrogen atoms were placed in calculated, ideal positions and refined as riding on their respective carbon atoms. Electron density contributions from disordered guest molecules were handled using the SQUEEZE procedure from the PLATON software suit[6]. Selected crystal data for **UCY-13** and **UCY-14** are summarized in Table S1. CCDC 1945717 (**UCY 13**) and 1945716 (**UCY 14**) contains the supplementary crystallographic data for this paper. Full details can be found in the CIF files provided as Supplementary Information.

Table S1. Selected Crystal Data for **UCY-13** and **UCY-14**.

Empirical formula	$C_{34}H_{16}O_{16}F_{12}Zr_3$	$C_{57}H_{33}O_{36}Zr_6$
Formula weight	1182.13	1841.15
Temperature	104(1) K	103(1) K
Wavelength	1.54184 Å	1.54184 Å
Crystal system	Monoclinic	Monoclinic
Space group	C 2/m	C 2/c
Unit cell dimensions	a = 14.5970(3) Å, α = 90° b = 30.6607(5) Å, β = 103.286(2)° c = 17.4140(3) Å, γ = 90°	a = 29.3698(8) Å, α = 90° b = 19.3135(7) Å, β = 97.510(3)° c = 19.0909(6) Å, γ = 90°
Volume	7585.1(2) $Å^3$	10736.1(6) $Å^3$
Z	4	4
Density (calculated)	1.035 g/cm^3	1.139 g/cm^3
Absorption coefficient	3.945 mm^{-1}	5.137 mm^{-1}
F(000)	2304	3612
Crystal size	0.041 x 0.036 x 0.01 mm^3	0.095 x 0.077 x 0.017 mm^3
θ range for data collection	3.429 to 66.994°	3.731 to 66.993°
Index ranges	-11<=h<=17, -34<=k<=36, -20<=l<=20	-35<=h<=21, -22<=k<=23, -22<=l<=21
Reflections collected	25792	19999
Independent reflections	6904 [R_{int} = 0.0328]	9539 [R_{int} = 0.0516]
Completeness to θ = 66.994°	99.8%	99.7%
Refinement method	Full-matrix least-squares on F^2	Full-matrix least-squares on F^2
Data / restraints / parameters	6904 / 0 / 303	9539 / 15 / 447
Goodness-of-fit	1.023	1.089
Final R indices [I > 2σ(I)]	R_{obs}^a = 0.0411, wR_{obs}^b = 0.1281	R_{obs}^a = 0.0849, wR_{obs}^b = 0.2506
R indices [all data]	R_{all} = 0.0470, wR_{all} = 0.1323	R_{all} = 0.0966, wR_{all} = 0.2639
Largest diff. peak and hole	1.732 and -0.771 $e \cdot Å^{-3}$	2.958 and -1.349 $e \cdot Å^{-3}$

[a] $R = \Sigma||F_o|-|F_c|| / \Sigma|F_o|$, $wR = \{\Sigma[w(|F_o|^2 - |F_c|^2)^2] / \Sigma[w(|F_o|^4)]\}^{1/2}$ and
[b] $w=1/[\sigma^2(Fo^2)+(mP)^2+nP]$ where $P=(Fo^2+2Fc^2)/3$ and m and n are constants.

Gas sorption measurements. Low Pressure gas sorption measurements were carried out at different temperatures using an Autosorb-iQ2 by Quantachrome equipped with a cryocooler system capable of temperature control from 20 to 320K. Prior to analysis the as made samples were washed with N,N- dimethylformamide four times per day for 1 day and then soaked in acetone 5 times per day for 5 days. Finally, the wet samples were transferred to 6mm sample cells and activated under dynamic vacuum at room temperature for 18 hours until the outgas rate was less than 2mTorr/min. After evacuation the samples were weighed to obtain the precise mass of the evacuated sample and the cells were transferred to the analysis port of the gas sorption instrument.

Uranyl sorption measurements. Uranyl sorption experiments were performed as reported elsewhere.[7] Specifically, the experiments were carried out at room temperature (23 ± 2 ^oC) under normal atmospheric conditions in 0.1 M $NaClO_4$ aqueous solutions. The preparation of the test solutions involved dissolution of an appropriate amount of a U(VI) stock solution (0.1 M) that was prepared by dissolution of $UO_2(NO_3)_2{\cdot}6H_2O$ in distilled water. Generally, test solutions (30 ml) containing U(VI) of known concentration, were mixed with a given mass of MOF and the resulting suspension was shaken in a thermostated orbital shaker (at 100 rpm) for 2 h to assure that equilibrium had been reached. Specifically, the effect of pH was studied in the pH range between 1 and 5, at constant U(VI) concentration ($[U(VI)]_o = 5*10^{-4}$ M) in the suspension and T = 296 K. The effect of ionic strength was studied by varying the $NaClO_4$ concentration between 0 and 0.5 M, at constant U(VI) concentration ($[U(VI)]_o = 5*10^{-4}$ M) in the suspension and T = 296 K. For studying the effect of initial U(VI) concentration, the latter was varied between 10^{-5} and $9*10^{-3}$ M in the test suspensions (0.033g of MOF in 30 ml solution) at pH 3. For kinetic studies certain amount of MOF (0.033 g) was mixed with 100 ml of U(VI) solutions ($[U(VI)]_o = 5*10^{-3}$ M, T = 296 K for **UCY-13** and ($[U(VI)]_o = 5*10^{-4}$ M, T = 296 K for **UCY-14**) at pH 3 and the metal concentration was determined at regular time steps. For the uranium analysis, aliquots collected from the suspension were filtered with membrane filters (pore size: 450 nm) and the uranium concentration was determined spectrophoto-metrically (UV 2401 PC Shimadzu) by means of arsenazo-III, according to a previously described method.[8]

Selectivity measurements. Uranyl selectivity sorption experiments were performed in 10 ml aqueous solutions of NaCl, $NaNO_3$, Na_2SO_4, $CaCl_2$ and commercial mineral water (CMW) spiked with 1 ppm of $UO_2(O_2CMe)_2{\cdot}6H_2O$ containing 10 mg of solid **UCY-13** or **UCY-14**. The solutions were left under magnetic stirring for 10 min and then the amount of remaining UO_2^{2+} was determined via AdSV (adsorptive stripping voltammetry). The voltammetric measurements were performed using a Trace Metal Analyzer (797 VA Computrace, Metrohm AG Ltd, Switzerland) equipped with a three-electrode system. Measurements were carried out in a 10 ml glass voltammetric cell equipped with Ag/AgCl/KCl (3 mol/L) as reference electrode and a Pt wire auxiliary electrode. The working electrode was Hanging Mercury Drop Electrode (HMDE). The analysis has been done following the AN-V-088 protocol developed by Metrohm (http://rohs.metrohm.com/Voltammetry/MVA2.html?identifier=AN-V-088&language=en).

Uranyl sorption studies from wastewater, simulated seawater, real seawater and ground water. Experiments of uranyl sorption from wastewater (WW) (from a local wastewater treatment plant), simulated seawater (SSW), real seawater (RSW) spiked with 1 ppm of UO_2^{2+} and ground water (GW) by **UCY-13** and **UCY-14** were performed. The determination of remaining uranium in solution was carried out by alpha-spectroscopy as described elsewhere.[9] In particular, investigations of uranyl sorption from local ground water known to exhibit a fairly high UO_2^{2+} concentration (~40 ppb)[10] involved addition of 0.1 g of as synthesized **UCY-13** and **UCY-14** to 200 ml of the aqueous samples and investigation of the uranium sorption under ambient conditions. In addition, SSW, RSW and WW samples were investigated by contacting 30 ml of the samples, which were contaminated with uranium standard reference solution, with 0.1 g of the MOF adsorbents. The contact time between the metal ions and the adsorbent was set at 3 hours to reach equilibrium. The experiments were repeated with similar samples traced with ^{232}U-tracer (NPL) or uranium AAS standard (Sigma Aldrich) solution to evaluate the method efficiency and simultaneously investigate the sorption process using spiked field samples.

Structural Figures

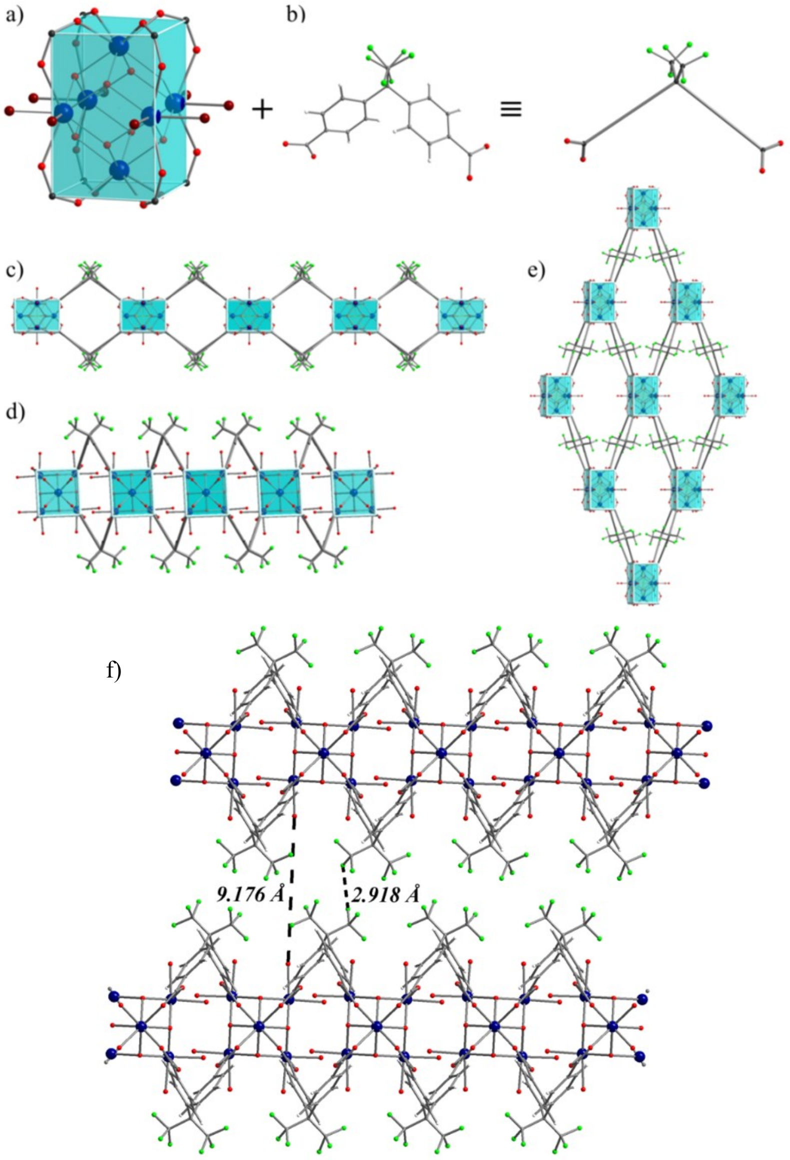

Figure S1: Representations of: a) the $[Zr_6(\mu_3\text{-}O)_4(\mu_3\text{-}OH)_4(COO)_8(OH)_4(H_2O)_4]$ SBU, b) the $HFPBBA^{2-}$ ligand as well as a simplified form in which the phenyl rings are omitted, c) the 2D framework along *a*-axis. d) the 2D framework along *b*-axis, e) the 2D framework along *c*-axis emphasizing on the formation of rhombic channels and f) the 2D framework along *b*-axis of **UCY-13**; dashed lines denote the closest distances between the SBUs and the intersheet hydrophobic interactions between two adjacent sheets. Color code: Zirconium, dark blue; Fluorine, light green; Oxygen, red; Carbon, grey; Hydrogen, white.

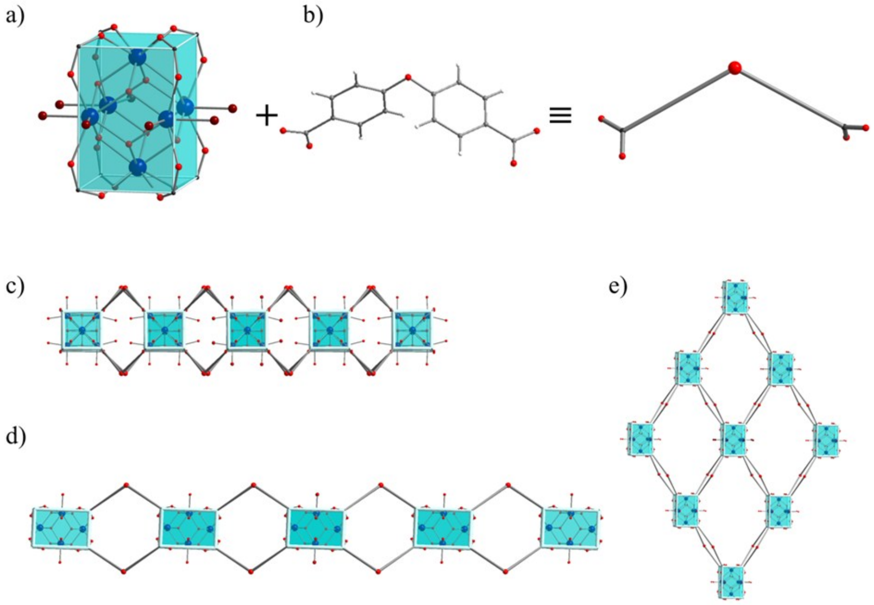

Figure S2: Representations of: a) the $[Zr_6(\mu_3\text{-}O)_4(\mu_3\text{-}OH)_4(COO)_8(OH)_4(H_2O)_4]$ cluster, b) the OBA^{2-} ligand as well as a simplified form in which the phenyl rings are omitted, c) the 2D framework along *a*-axis, d) the 2D framework along *b*-axis and e) the 2D framework along *c*-axis of **UCY-14** emphasizing on the formation of rhombic channels. Color code: Zirconium, dark blue; Oxygen, red; Carbon, grey; Hydrogen, white.

Physical Measurements/Characterization

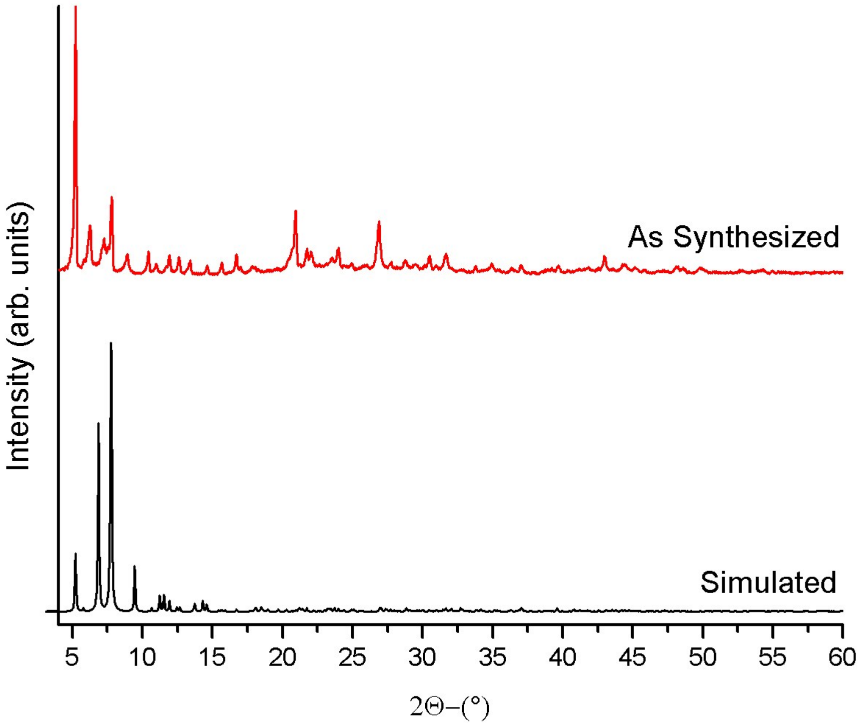

Figure S3: Powder X-ray diffraction pattern of the as synthesized compound **UCY-13**, along with the simulated pattern from the single crystal data.

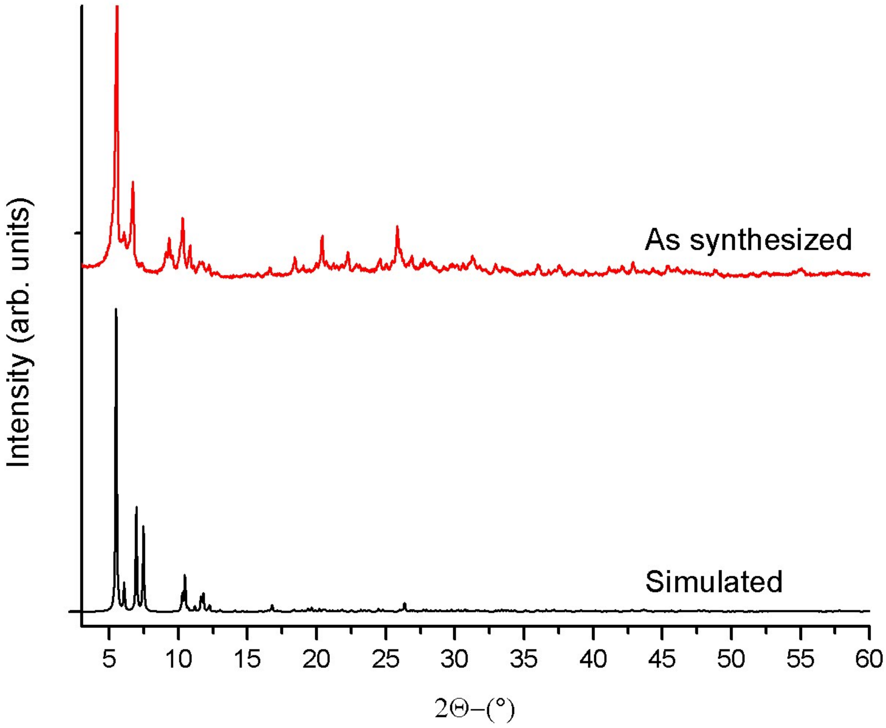

Figure S4: Powder X-ray diffraction pattern of the as synthesized compound **UCY-14**, along with the simulated pattern from the single crystal data.

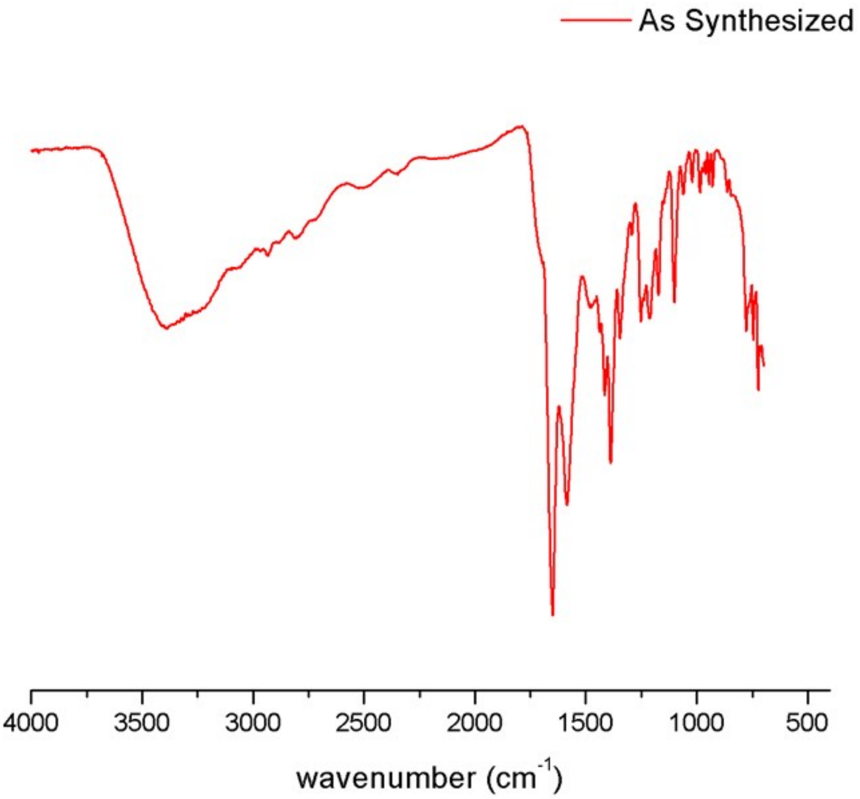

Figure S5: IR spectrum of the as synthesized compound **UCY-13**.

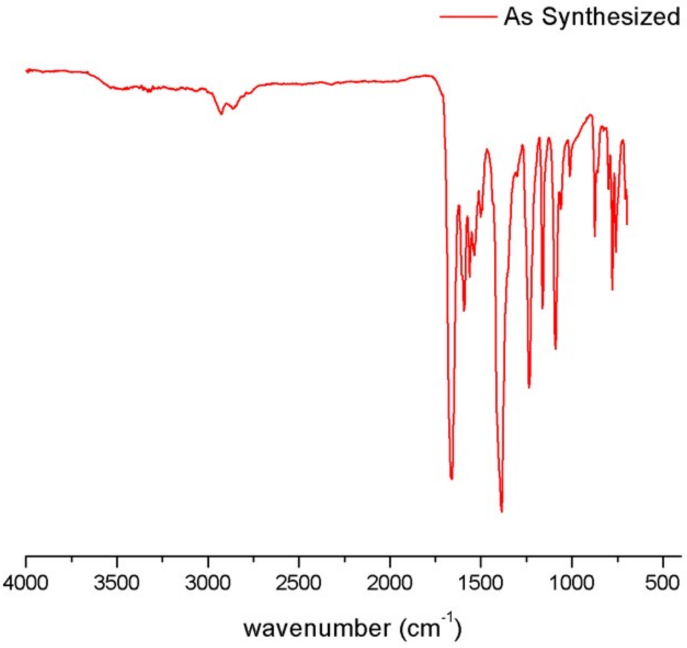

Figure S6: IR spectrum of the as synthesized compound **UCY-14**.

Stability Studies

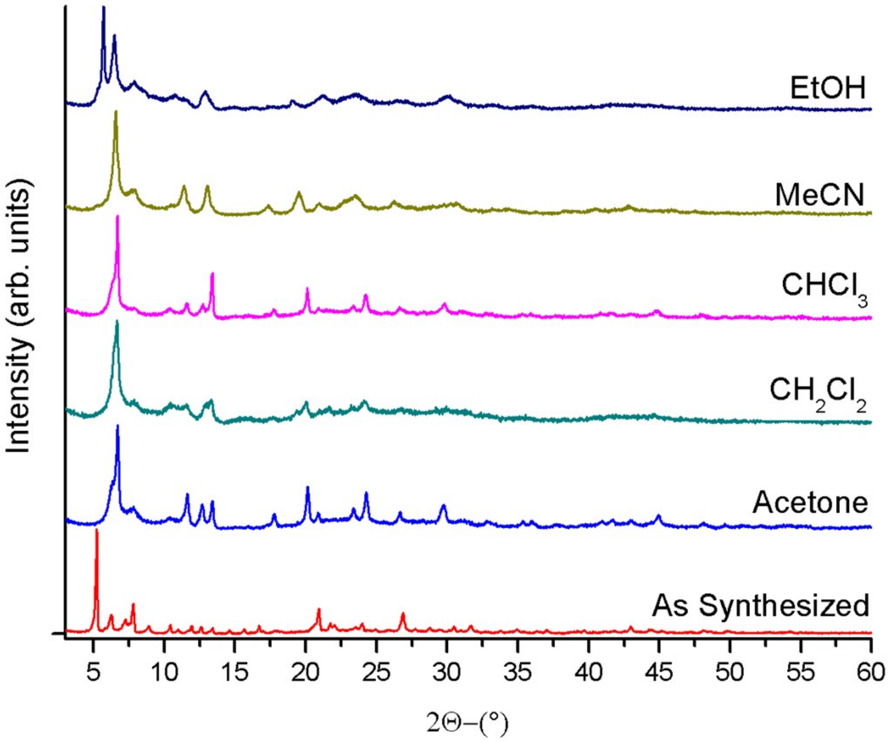

Figure S7: Powder X-ray diffraction patterns of **UCY-13** treated (as described in the experimental part) in the indicated organic solvents.

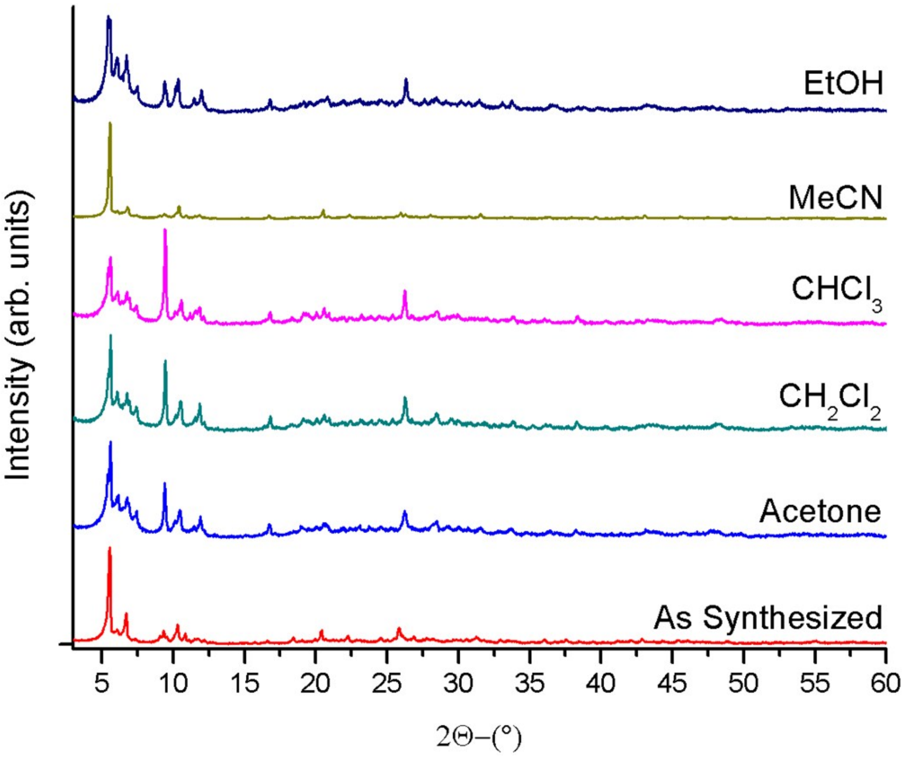

Figure S8: Powder X-ray diffraction patterns of **UCY-14** treated (as described in the experimental part) in the indicated organic solvents.

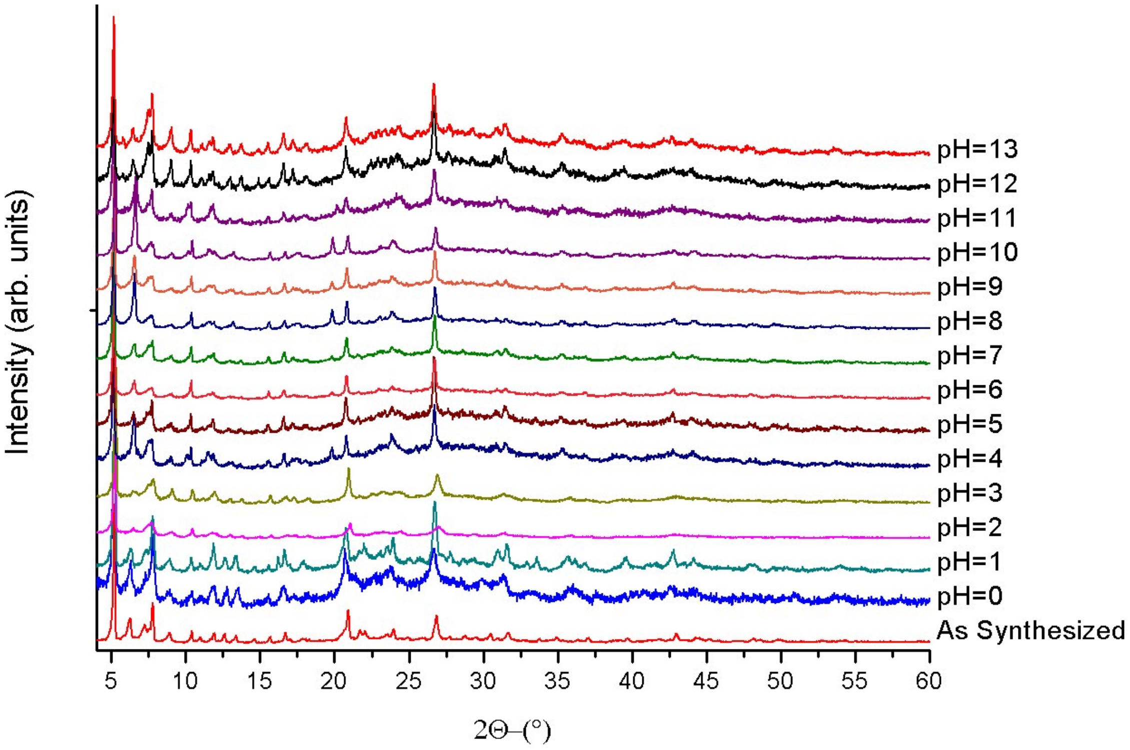

Figure S9: Powder X-ray diffraction patterns of **UCY-13** treated (as described in the experimental part) in aqueous solutions of the indicated pH values.

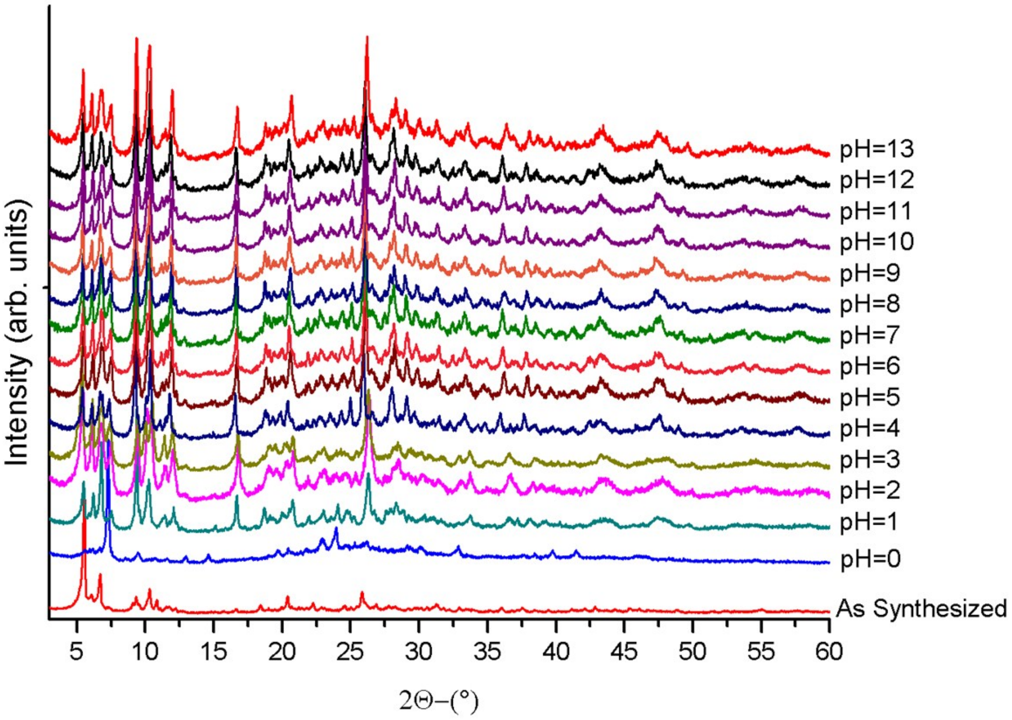

Figure S10: Powder X-ray diffraction patterns of **UCY-14** treated (as described in the experimental part) in aqueous solutions of the indicated pH values.

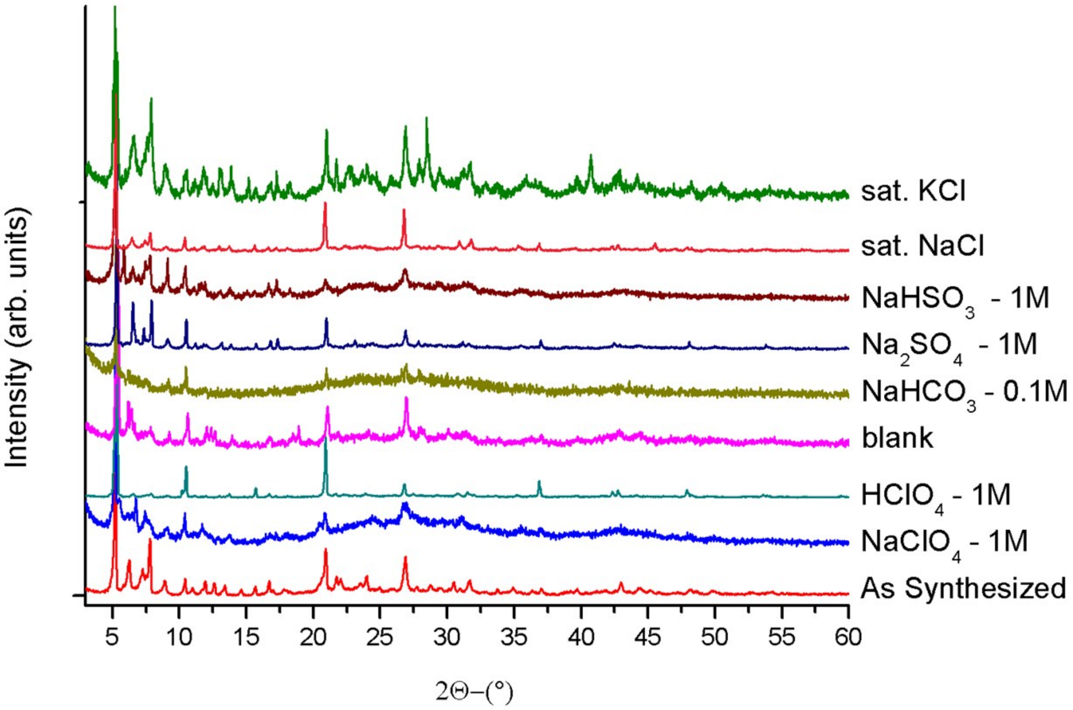

Figure S11: Powder X-ray diffraction patterns of **UCY-13** treated (as described in the experimental part) in aqueous solutions of the indicated chemical species. Blank: 0.1M $NaClO_4$ and $NaNO_3$ 0.5mM.

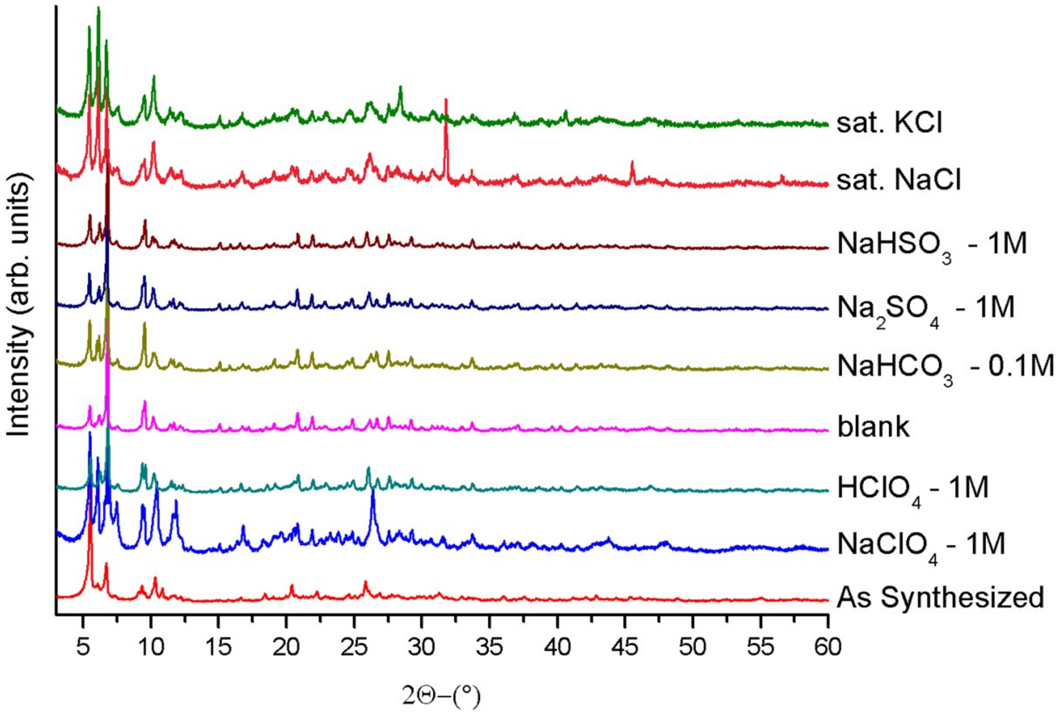

Figure S12: Powder X-ray diffraction patterns of **UCY-14** treated (as described in the experimental part) in aqueous solutions of the indicated chemical species. Blank: 0.1M $NaClO_4$ and $NaNO_3$ 0.5mM.

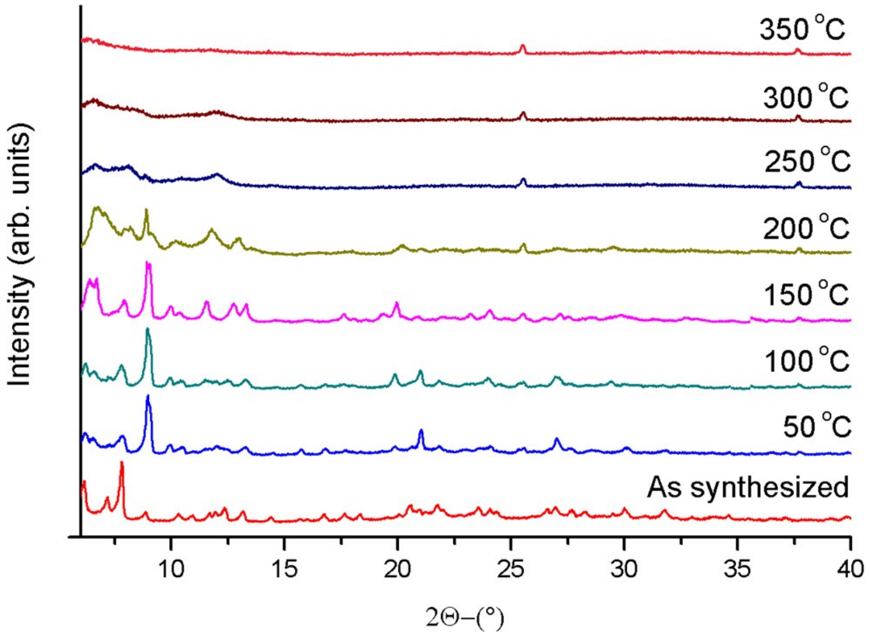

Figure S13: Variable temperature pXRD patterns of compound **UCY-13**.

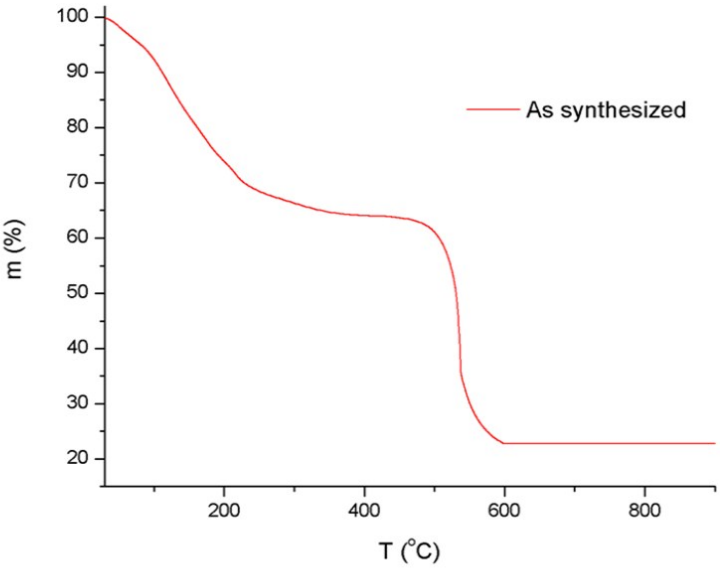

Figure S14: TGA graph of the as synthesized compound **UCY-13**. TG analysis reveals that the thermal decomposition of compound **UCY-13** proceeds via a two-step process. The first step (until ~450^{o}C) is attributed to the removal of the lattice DMF and HCOOH molecules and terminally ligated H_2O molecules corresponds to ~37.0 % of the material's total mass. This value is in agreement with the corresponding calculated value for **UCY-13**·8DMF·16HCOOH (~37.6%). In fact, ^{1}H-NMR measurements of the digested (in aq.KOH) as synthesized material also support the presence of DMF and HCOOH molecules in **UCY-13** (Fig. S15). The second mass loss which is completed at ~600^{o}C is attributed to the decomposition of the ligand HFPBBA^{2-} and accounts to ~41.5 % of the initial mass of the compound (calculated for **UCY-13**·8DMF·16HCOOH ~42.2%).

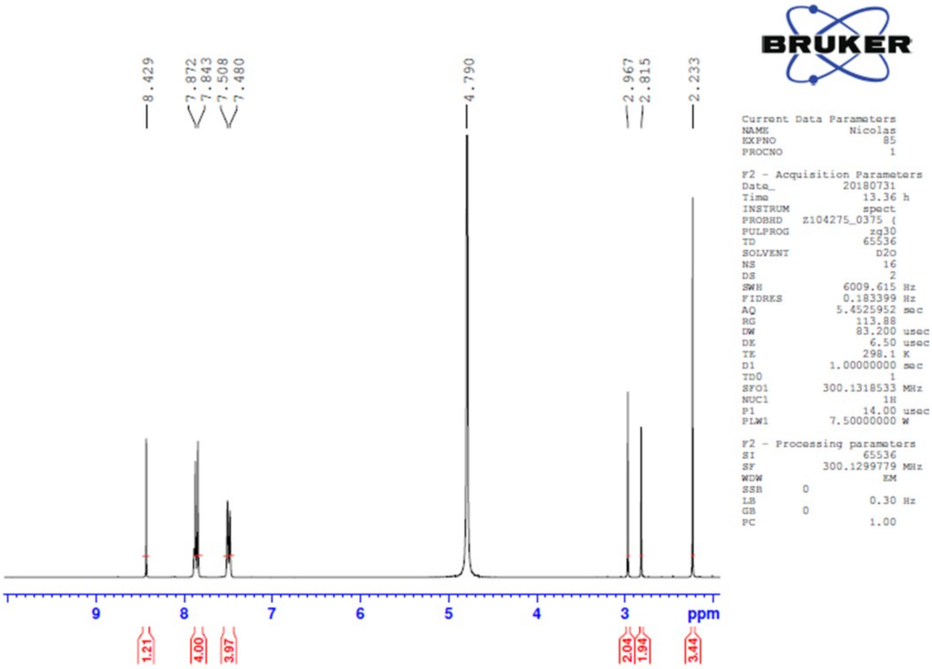

```
Current Data Parameters
NAME              Nicolas
EXPNO                  85
PROCNO                  1

F2 - Acquisition Parameters
Date_            20180731
Time                13.36 h
INSTRUM             spect
PROBHD   Z104275_0375 (
PULPROG              zg30
TD                  65536
SOLVENT               D2O
NS                     16
DS                      2
SWH              6009.615 Hz
FIDRES           0.183399 Hz
AQ              5.4525952 sec
RG                 113.88
DW                 83.200 usec
DE                   6.50 usec
TE                  298.1 K
D1             1.00000000 sec
TD0                     1
SFO1          300.1318533 MHz
NUC1                   1H
P1                  14.00 usec
PLW1           7.50000000 W

F2 - Processing parameters
SI                  65536
SF            300.1299779 MHz
WDW                    EM
SSB        0
LB                   0.30 Hz
GB         0
PC                   1.00
```

Figure S15: ^{1}H-NMR spectrum of as synthesized **UCY-13** digested in 0.5M KOH in D_2O. These data indicate the presence of the organic ligand HFPBBA^{2-} as well as HCOOH and DMF in **UCY-13**. ^{1}H NMR (D_2O): δ 2.233 (s, 6H, C**H$_3$**, Acetone), δ 2.815 (s, 3H, C**H$_3$**, DMF), δ 2.967 (s, 3H, C**H$_3$**, DMF), δ 4.790 (s, 2H, **H$_2$**O, H_2O), δ 7.494 (d, 4H, Ar-**H**, HFPBBA^{2-}), δ 7.857 (d, 4H, Ar-**H**, HFPBBA^{2-}), δ 8.429 (s, 1H, **H**COO$^-$, HCOO$^-$).

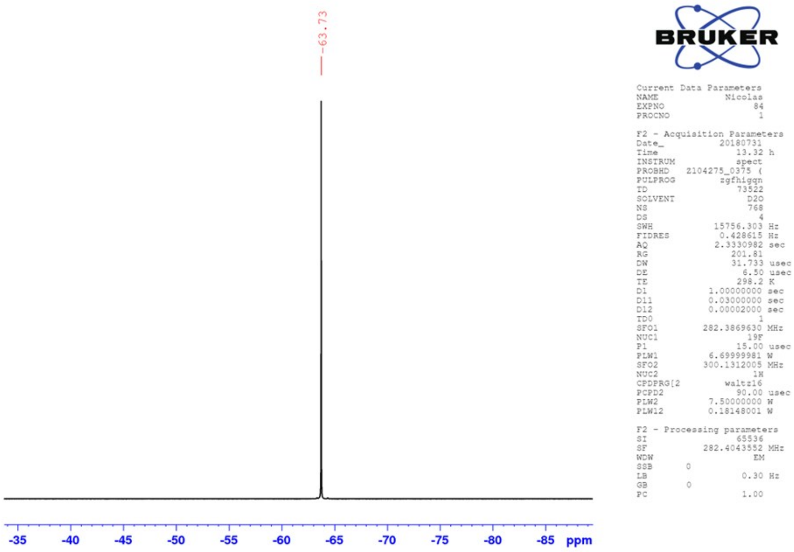

```
Current Data Parameters
NAME              Nicolas
EXPNO                  84
PROCNO                  1

F2 - Acquisition Parameters
Date_            20180731
Time                13.32 h
INSTRUM             spect
PROBHD   Z104275_0375 (
PULPROG           zgfhigqn
TD                  73522
SOLVENT               D2O
NS                    768
DS                      4
SWH             15756.303 Hz
FIDRES           0.428615 Hz
AQ              2.3330982 sec
RG                 201.81
DW                 31.733 usec
DE                   6.50 usec
TE                  298.2 K
D1             1.00000000 sec
D11            0.03000000 sec
D12            0.00002000 sec
TD0                     1
SFO1          282.3869630 MHz
NUC1                  19F
P1                  15.00 usec
PLW1           6.69999981 W
SFO2          300.1312005 MHz
NUC2                   1H
CPDPRG[2          waltz16
PCPD2               90.00 usec
PLW2           7.50000000 W
PLW12          0.18148001 W

F2 - Processing parameters
SI                  65536
SF            282.4043552 MHz
WDW                    EM
SSB        0
LB                   0.30 Hz
GB         0
PC                   1.00
```

Figure S16: ^{19}F-NMR spectrum of as synthesized **UCY-13** digested in 0.5M KOH in D_2O. These data indicate the presence of the organic ligand HFPBBA^{2-} in **UCY-13**.

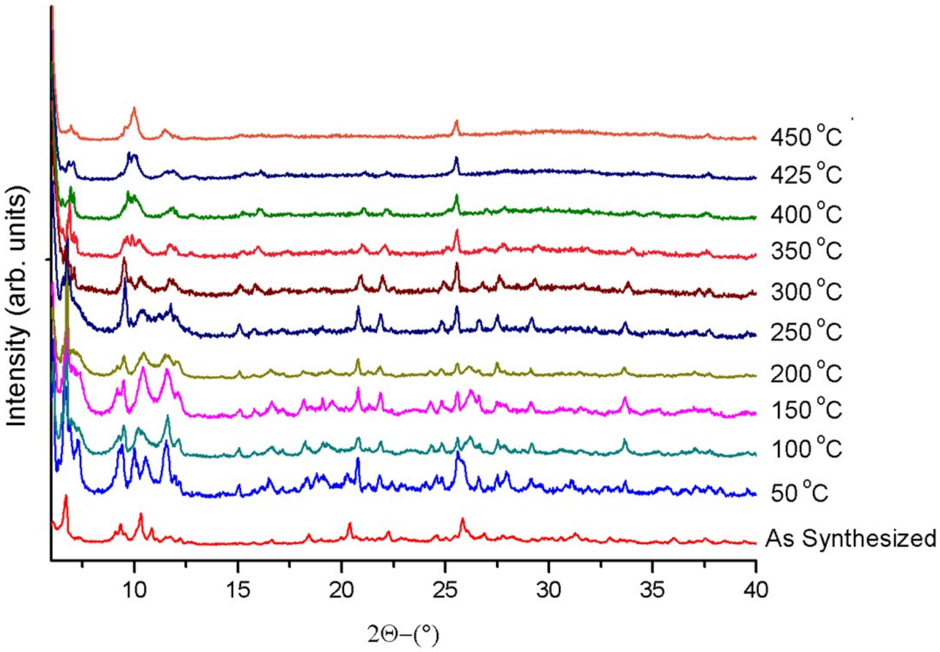

Figure S17: Variable temperature pxrd patterns of compound **UCY-14**.

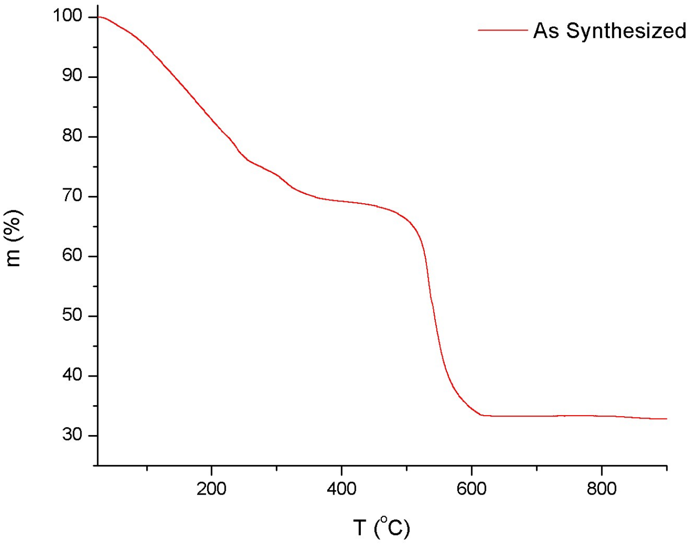

Figure S18: TGA graph of the as synthesized compound **UCY-14**. TG analysis reveals that the thermal decomposition of compound **UCY-14** proceeds via a two-step process. The first step (until ~450°C) is attributed to the removal of the lattice / coordinated HCOOH groups and lattice DMF molecules and corresponds to ~30.8 % of material's total mass. This value is in agreement with the corresponding calculated value for **UCY-14**·6DMF·6HCOOH (~30%). In fact, ^{1}H-NMR measurements of the digested (in aq.KOH) as synthesized material also support the presence of DMF and HCOOH molecules in **UCY-14** (Fig. S19). The second mass loss is completed at ~600°C and is attributed to the decomposition of the ligand OBA^{2-} which accounts to 38 % of the initial mass of compound **UCY-14**·6DMF·6HCOOH (calculated 39.5 %).

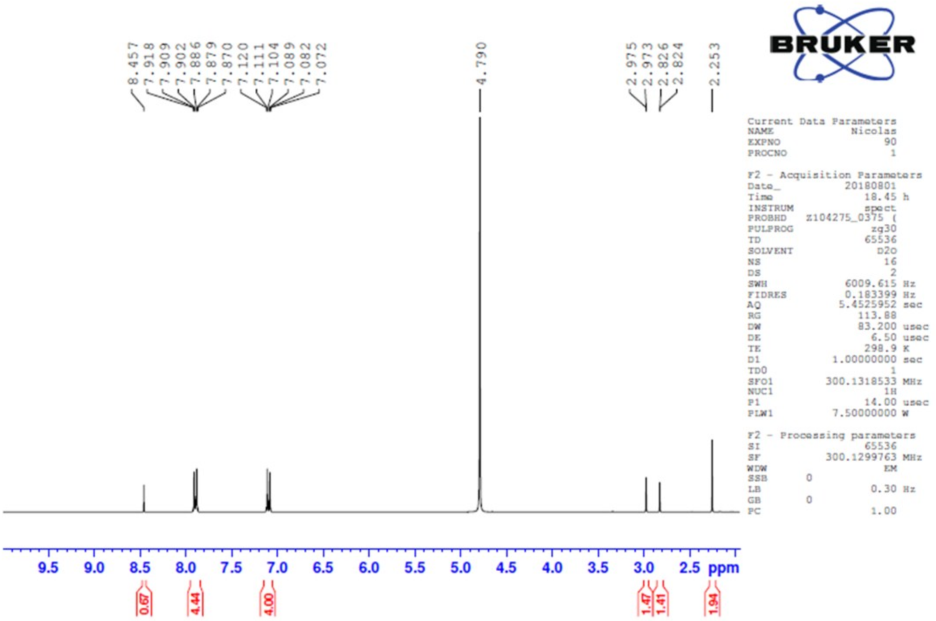

```
Current Data Parameters
NAME             Nicolas
EXPNO                 90
PROCNO                 1

F2 - Acquisition Parameters
Date_           20180801
Time               18.45 h
INSTRUM            spect
PROBHD   Z104275_0375 (
PULPROG             zg30
TD                 65536
SOLVENT              D2O
NS                    16
DS                     2
SWH             6009.615 Hz
FIDRES          0.183399 Hz
AQ             5.4525952 sec
RG                113.88
DW                83.200 usec
DE                  6.50 usec
TE                 298.9 K
D1            1.00000000 sec
TD0                    1
SFO1         300.1318533 MHz
NUC1                  1H
P1                 14.00 usec
PLW1          7.50000000 W

F2 - Processing parameters
SI                 65536
SF           300.1299763 MHz
WDW                   EM
SSB      0
LB                  0.30 Hz
GB       0
PC                  1.00
```

Figure S19: ^{1}H-NMR spectrum of as synthesized **UCY-14** digested in 0.5M KOH in D_2O. These data indicate the presence of the organic ligand OBA^{2-} as well as HCOOH and DMF in **UCY-14**. ^{1}H NMR (D_2O): δ 2.253 (s, 6H, C**H_3**, Acetone), δ 2.825 (s, 3H, C**H_3**, DMF), δ 2.974 (s, 3H, C**H_3**, DMF), δ 4.790 (s, 2H, **H_2**O, H_2O), δ 7.096 (d, 4H, Ar-**H**, OBA^{2-}), δ 7.894 (d, 4H, Ar-**H**, OBA^{2-}), δ 8.457 (s, 1H, **H**COO^-, $HCOO^-$).

Gas Sorption Measurements

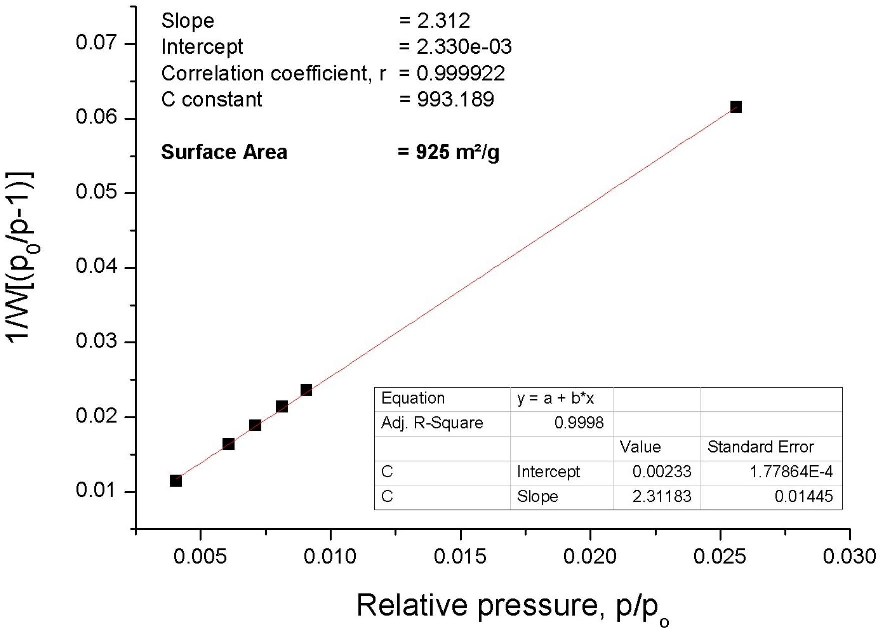

Figure S20: BET plot for the **UCY-13** from Ar adsorption isotherm at 87K.

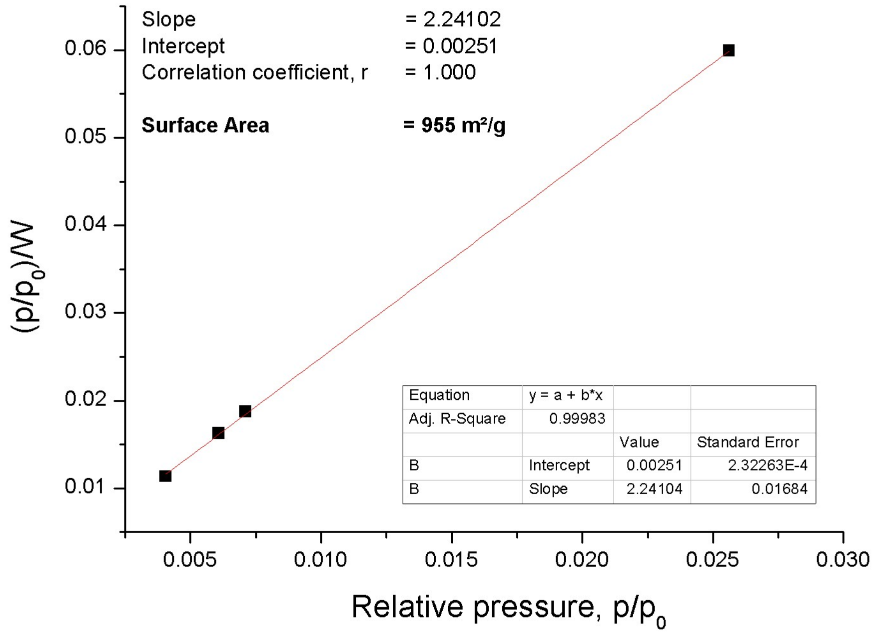

Figure S21: Langmuir plot for **UCY-13** from Ar adsorption isotherm at 87K.

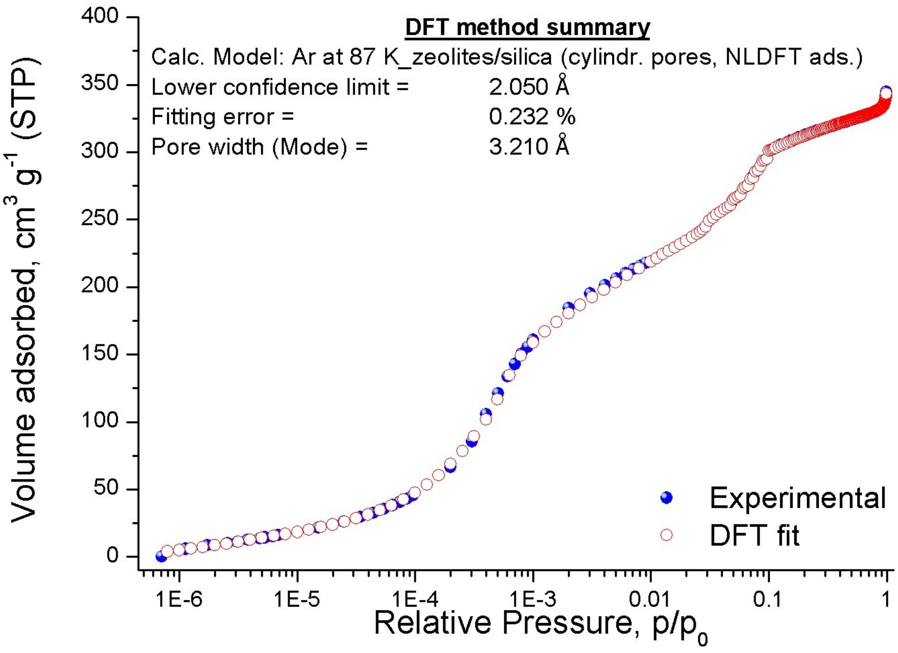

DFT method summary

Calc. Model: Ar at 87 K_zeolites/silica (cylindr. pores, NLDFT ads.)

Lower confidence limit = 2.050 Å

Fitting error = 0.232 %

Pore width (Mode) = 3.210 Å

Figure S22: Argon adsorption isotherm of **UCY-13** recorded at 87 K and the corresponding NLDFT fitting.

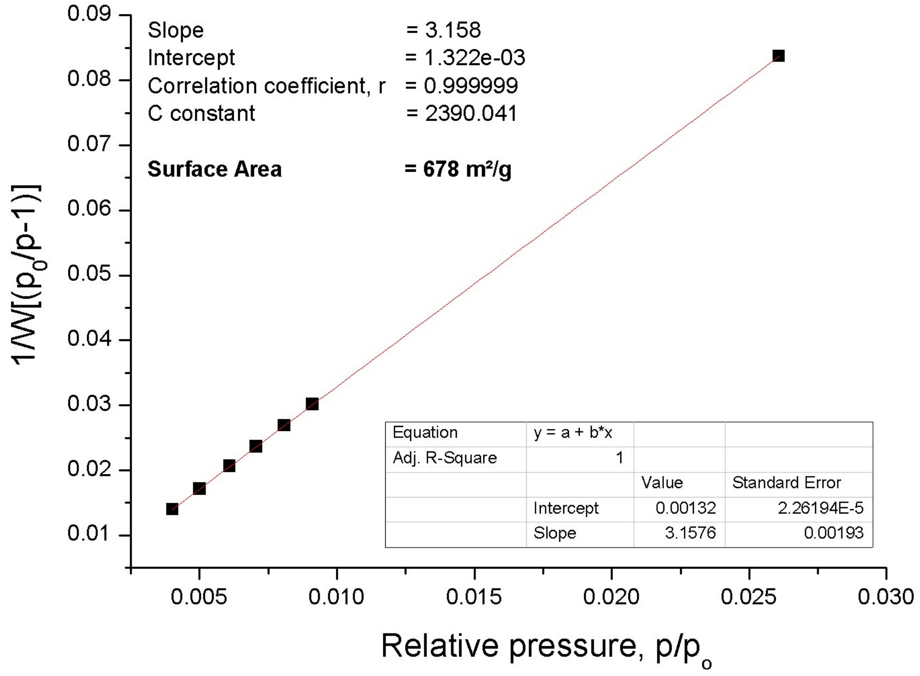

Slope = 3.158

Intercept = 1.322e-03

Correlation coefficient, r = 0.999999

C constant = 2390.041

Surface Area = 678 m²/g

Equation	y = a + b*x		
Adj. R-Square	1		
		Value	Standard Error
	Intercept	0.00132	2.26194E-5
	Slope	3.1576	0.00193

Figure S23: BET plot for the **UCY-14** from Ar adsorption isotherm at 87 K.

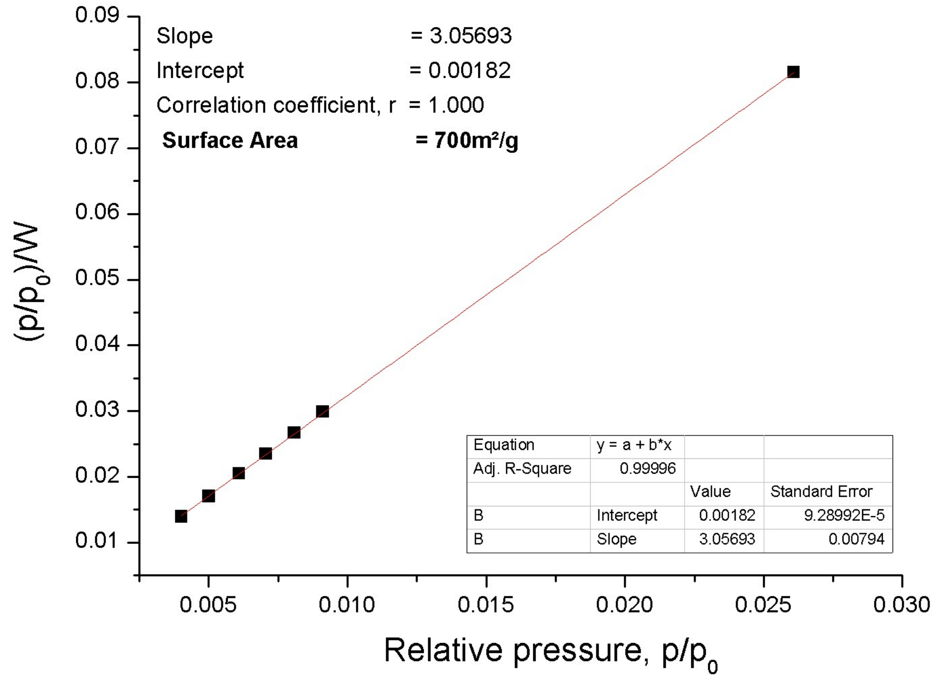

Figure S24: Langmuir plot for **UCY-14** from Ar adsorption isotherm at 87 K.

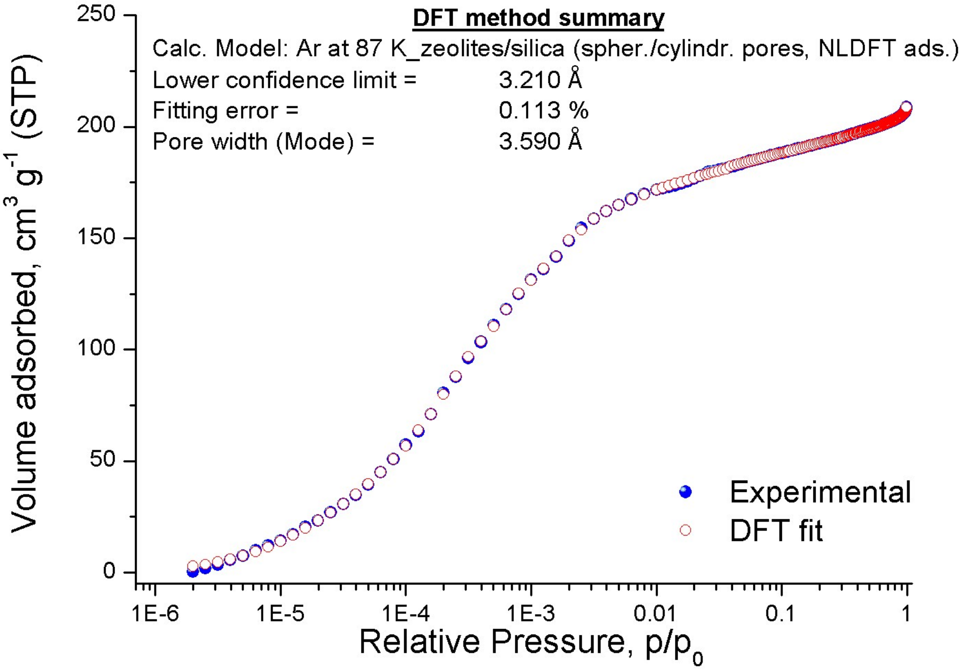

Figure S25: Argon adsorption isotherm of **UCY-14** recorded at 87 K and the corresponding NLDFT fitting.

Low pressure CO_2, CH_4 and H_2 sorption isotherms, determination of heat of adsorption and CO_2/CH_4 selectivity calculations using IAST.

Heat of adsorption: To calculate heats of adsorptions, the corresponding adsorption isotherms at two different temperatures (77 K / 87 K for H_2 and 273 K / 293 K for CO_2 and CH_4) were simultaneously fitted using the virial type[11,12] Equation 1:

$$\ln P = \ln N + \frac{1}{T}\sum_{i=0}^{m} a_i N^i + \sum_{i=0}^{n} b_i N^i \tag{1}$$

The heat of adsorption at zero coverage was calculated from Equation 2, where as a function of surface coverage, from Equation 3:

$$Q_{st} = -Ra_o \tag{2}$$

$$Q_{st}(N) = -R\sum_{i=0}^{m} a_i N^i \tag{3}$$

For the determination of the isosteric heat of adsorption using the Clausious - Clapeyron equation a commercially available software, ASiQwin (version 3.01) purchased from Quantachrome, was used.

Gas Selectivity using the IAST model. The corresponding calculations were performed according to an established procedure.[13–15] Specifically, the single-component adsorption isotherms were described by fitting the data with the following virial-type equation.

$$p = \frac{n}{K} exp(c_1 1n + c_2 n^2 + c_3 n^3 + c_4 n^4) \tag{4}$$

Where p is the pressure in Torr, n is the adsorbed amount in mmol g-1, K is the Henry constant in mmol g-1 Torr-1 and ci are the constants of the virial equation.

The free energy of desorption at a given temperature and pressure of the gas is obtained from the analytical integration of eq. (4):

$$G(T,p) = RT\int_0^p \frac{n}{p}dp = RT(n + \frac{1}{2}c_1n^2 + \frac{2}{3}c_2n^3 + \frac{3}{4}c_3n^4 + \frac{4}{5}c_4n^5) \qquad (5)$$

The free energy of desorption is a function of temperature and pressure G(T,p) and describes the minimum work (Gibbs free energy) that required to completely degas the adsorbent surface.

For a binary mixture of component i and j eq. (5) yields the individual pure loadings $n_i^0$and n_j^0 at the same free energy of desorption:

$$G_i^0(n_i^0) = G_j^0(n_j^0) \qquad (6)$$

The partial pressure of component i and j in an ideal adsorption mixture is given by the following equations:

$$py_i = p_i^0(n_i^0)x_i \qquad (7)$$

$$py_j = p_j^0(n_j^0)x_j \qquad (8)$$

whereyi (=1-yj) and xi (=1-xj) is the molar fraction of component i in the gas phase and the adsorbed phase respectively and p_i^0, $p_j^0$is the pure component pressure of i and j respectively. From eq. (6)-(8) and (3), the selectivity for the adsorbates i and j (Si,j) and the total pressure (p) of the gas mixture were calculated from eq. (9) and eq. (10), respectively.

$$S_{ij} = \frac{x_i/y_i}{x_j/y_j} = \frac{p_j^0}{p_i^o} \qquad (9)$$

$$p = \sum_i^j (p_i^o x_i) \qquad (10)$$

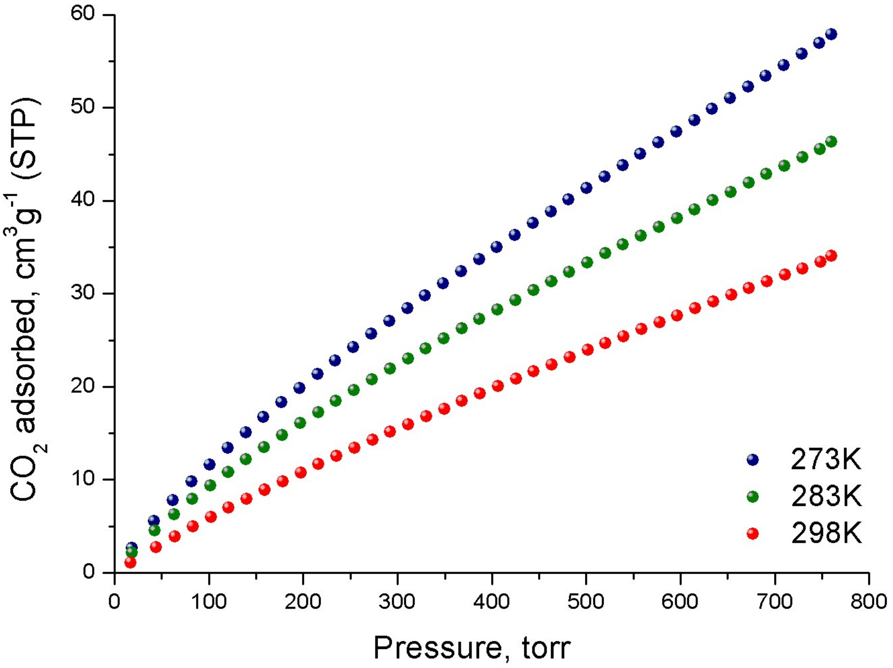

Figure S26: CO_2 adsorption isotherms of **UCY-13** at 273 K, 283 K and 298 K.

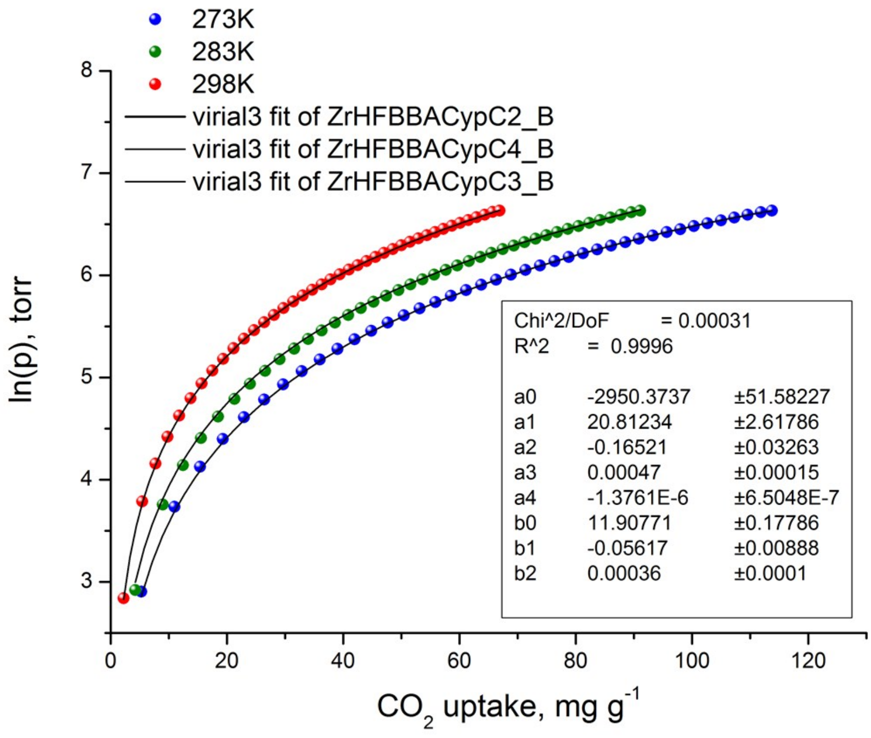

Figure S27: Virial type fitting of CO_2 adsorption isotherms of **UCY-13** at 273 K, 283 K and 298 K according to equation 1.

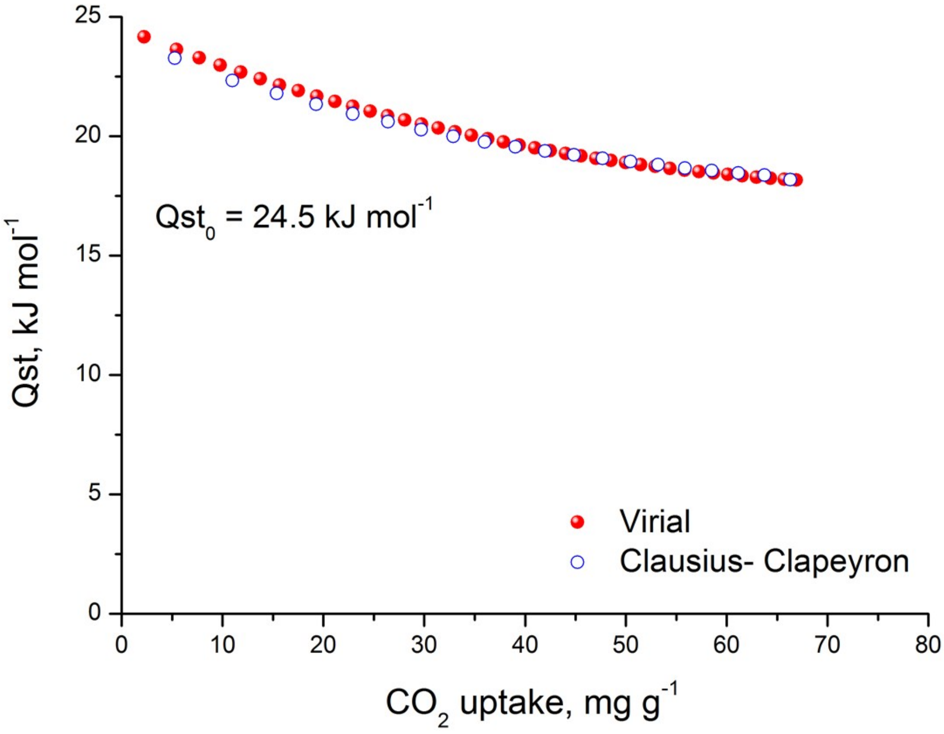

Figure S28: CO_2 isosteric heat of adsorption in **UCY-13** as a function of surface coverage.

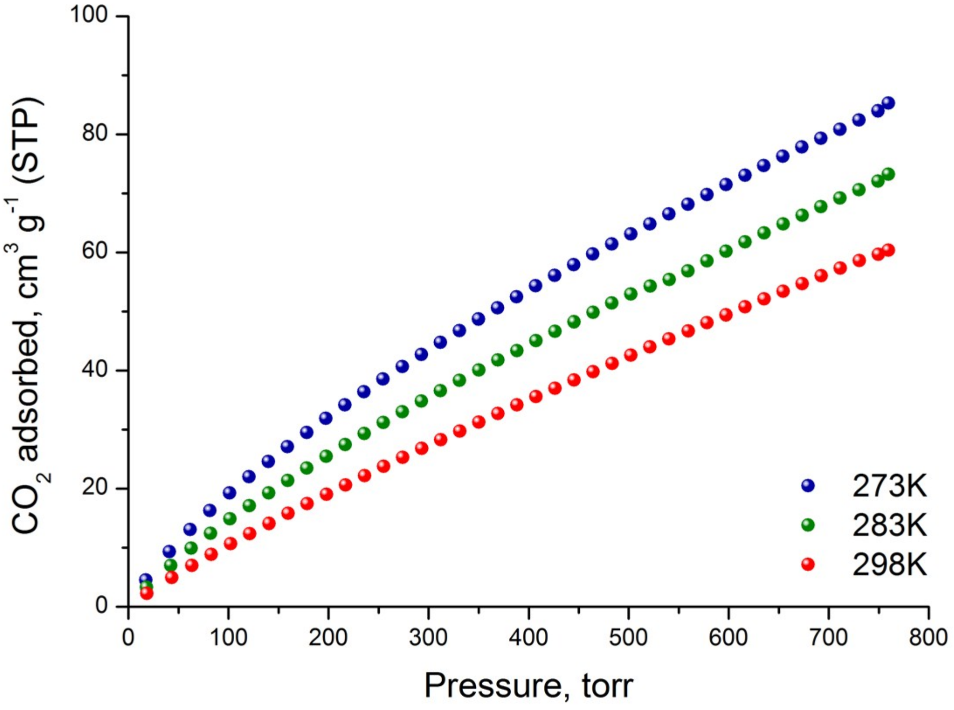

Figure S29: CO_2 Adsorption isotherms of **UCY-14** at 273 K, 283 K and 298 K.

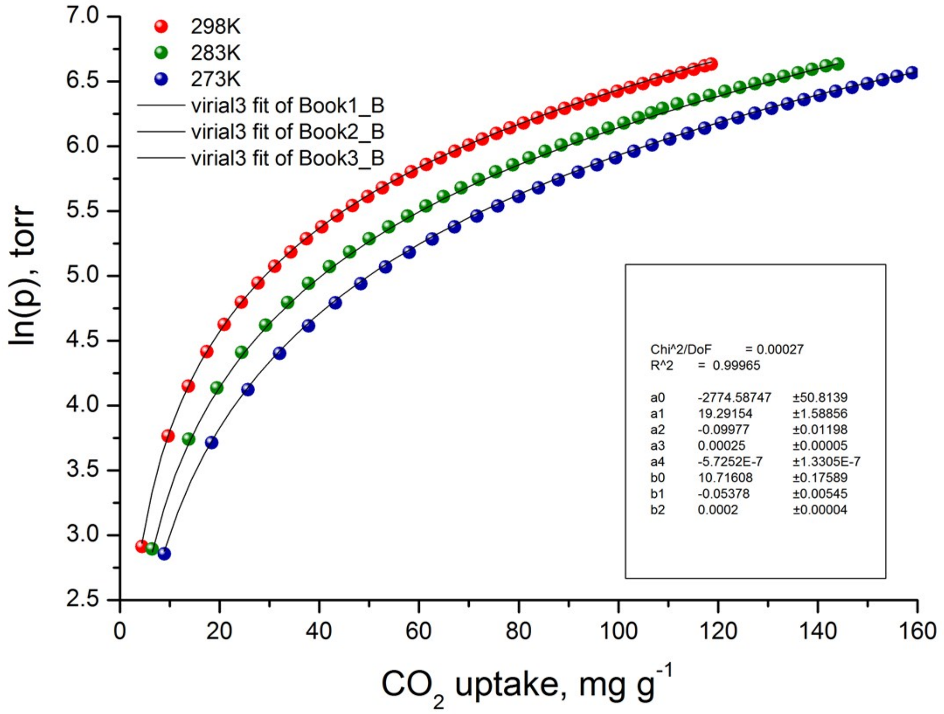

Figure S30: Virial type fitting of CO_2 adsorption isotherms of **UCY-14** at 273 K, 283 K and 298 K according to equation 1.

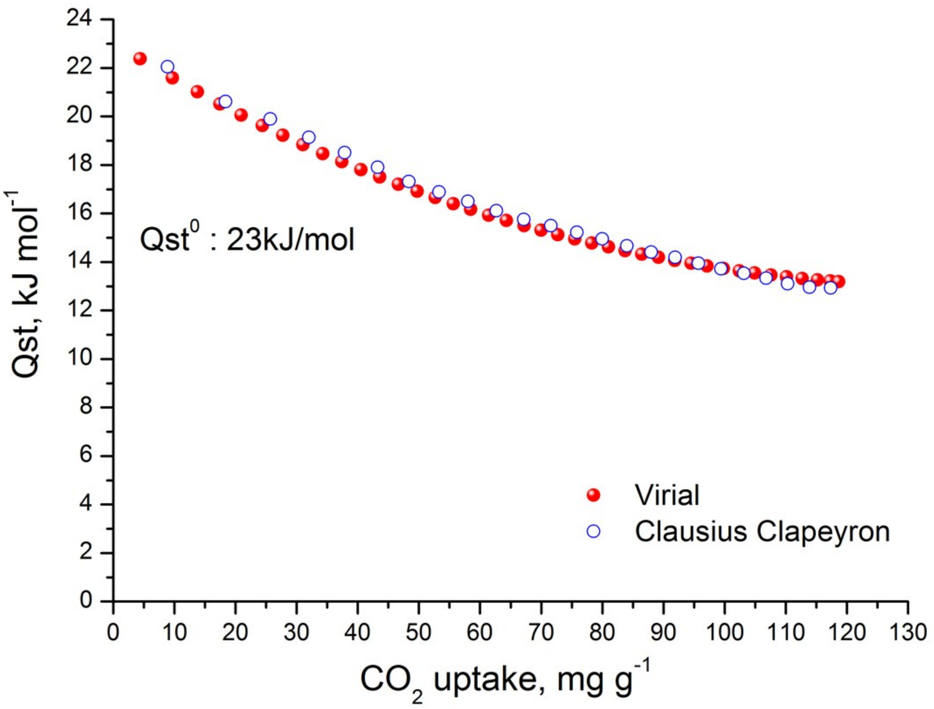

Figure S31: CO_2 isosteric heat of adsorption in **UCY-14** as a function of surface coverage.

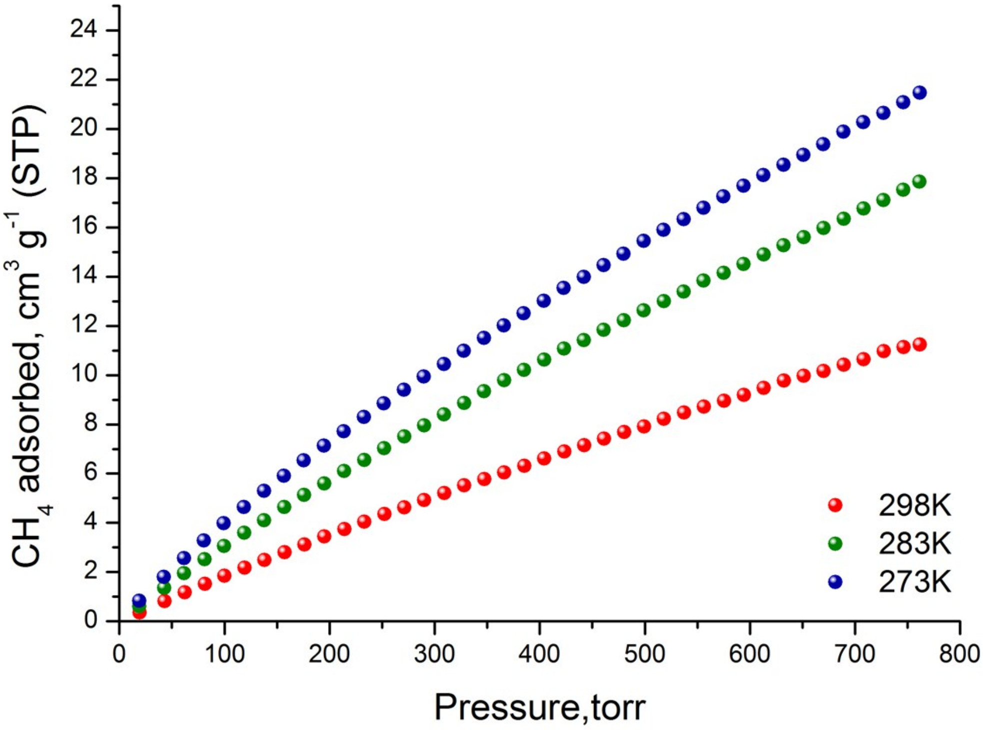

Figure S32: CH_4 adsorption isotherms of **UCY-13** at 273 K, 283 K and 298 K.

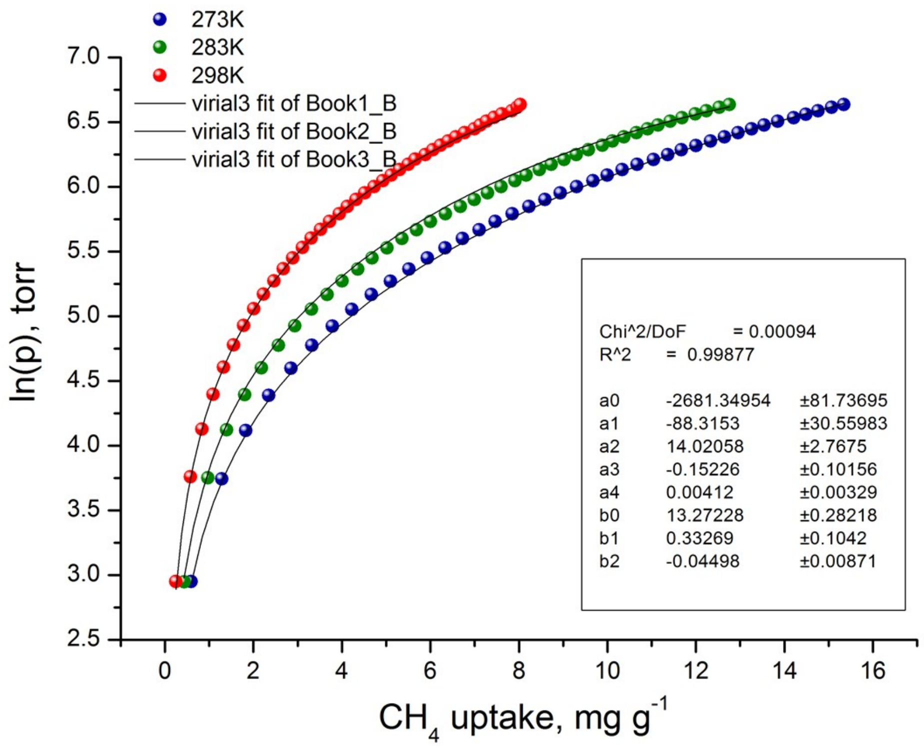

Figure S33: Virial type fitting of CH_4 adsoprtion isotherms of **UCY-13** at 273 K, 283 K and 298 K accornding to equation 1.

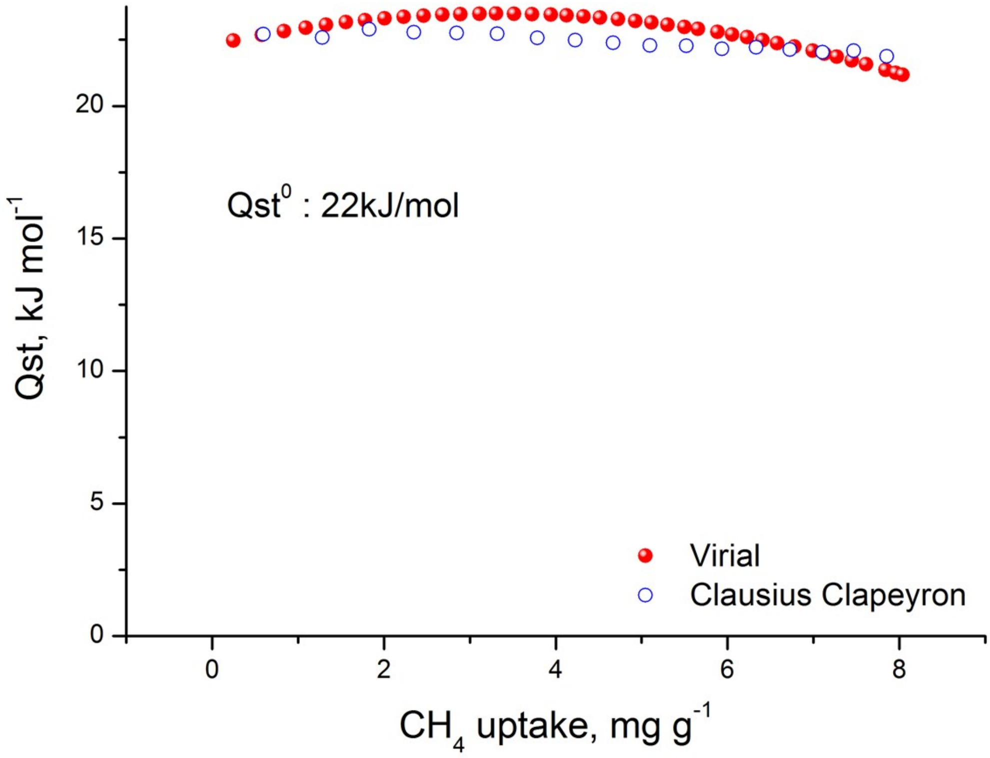

Figure S34: CH_4 isosteric heat of adsorption in **UCY-13** as a function of surface coverage.

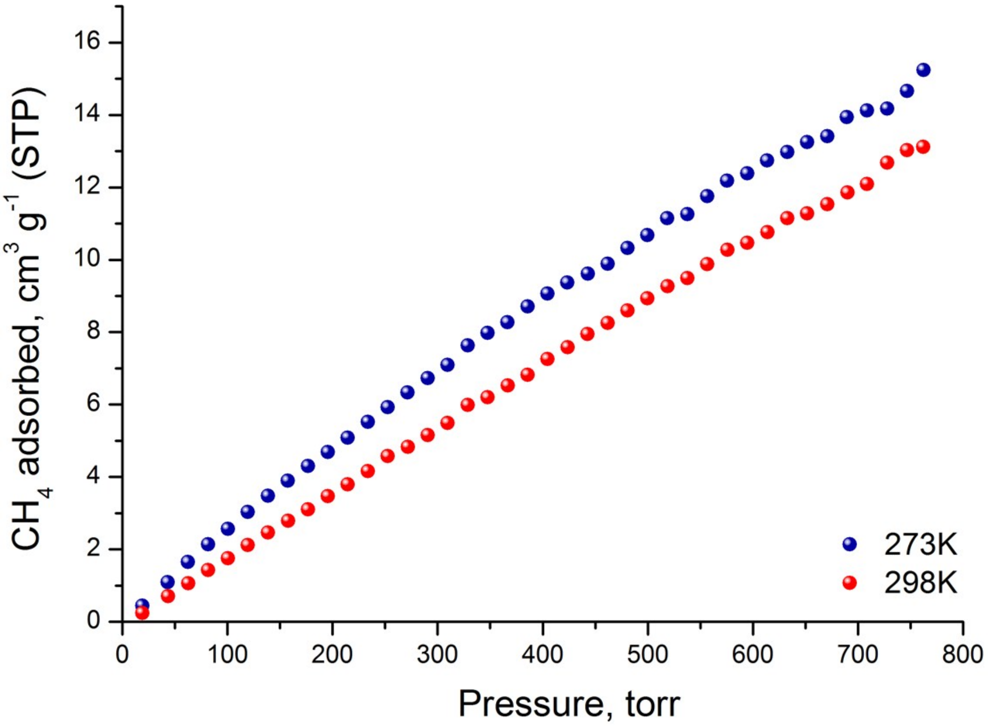

Figure S35: CH_4 adsorption isotherms of **UCY-14** at 273 K and 298 K.

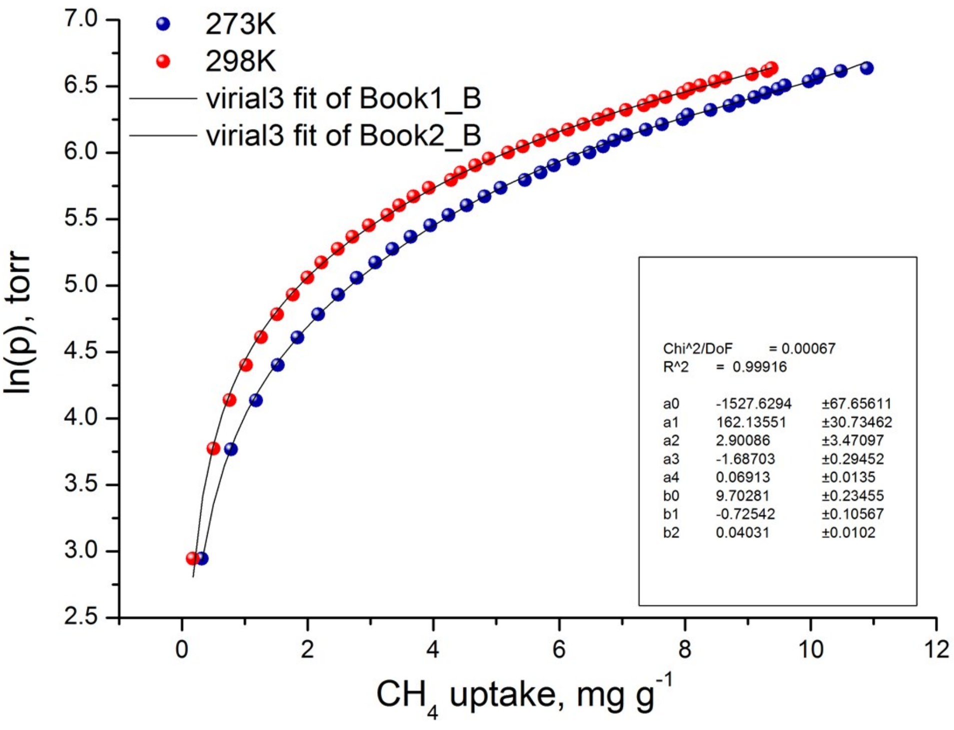

Figure S36: Virial type fitting of CH_4 adsorption isotherms of **UCY-14** at 273 K and 298 K according to equation 1.

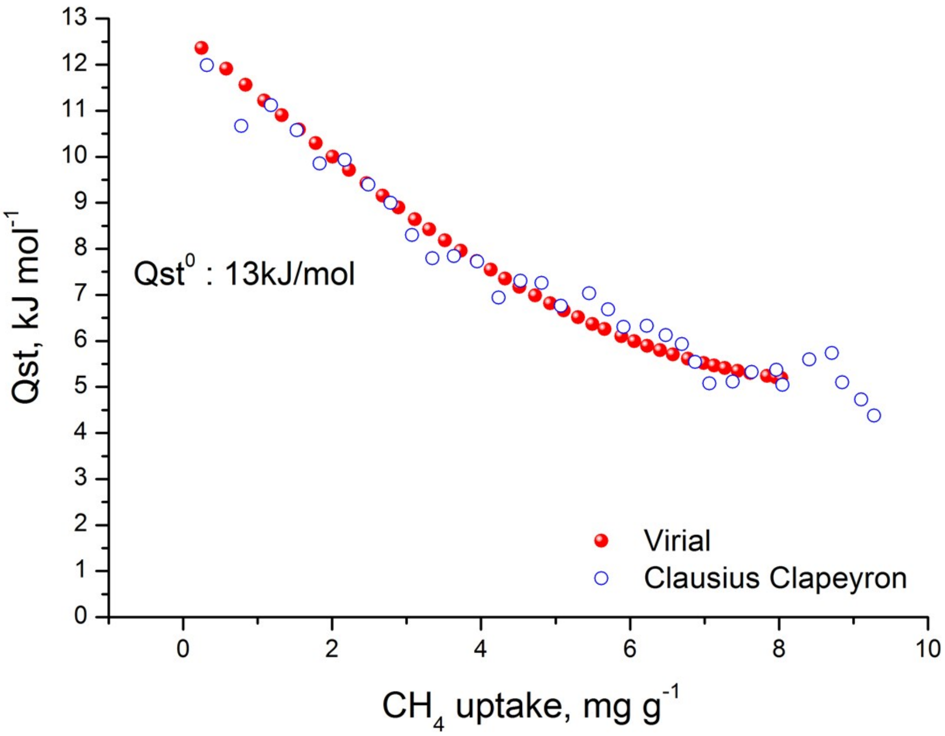

Figure S37: CH_4 isosteric heat of adsorption in **UCY-14** as a function of surface coverage.

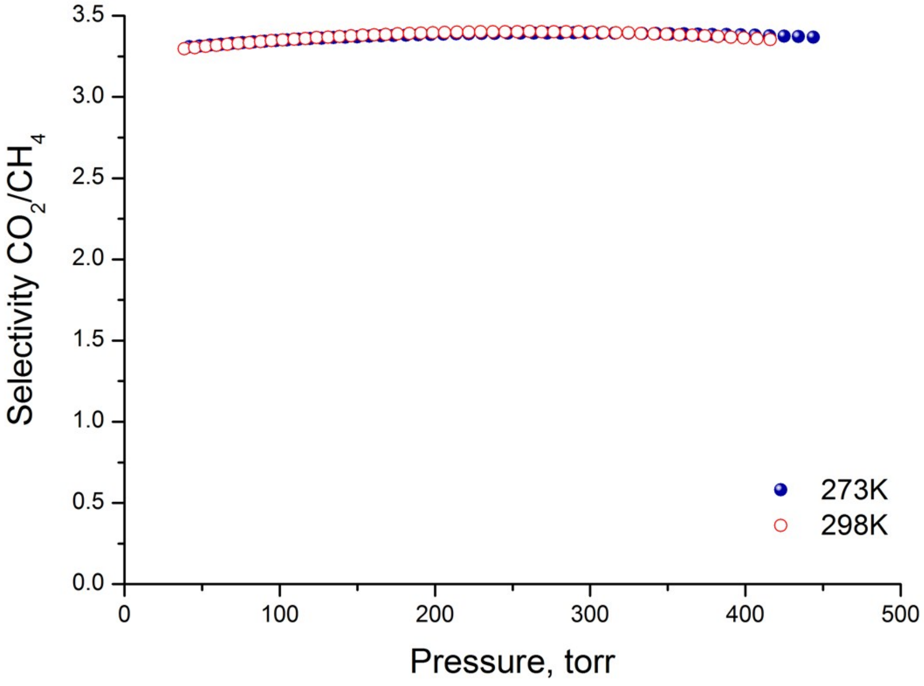

Figure S38: Selectivities of CO_2 over CH_4 at 298 K and 273 K for **UCY-13** as predicted by IAST for a 5/95 CO_2/CH_4 molar mixture.

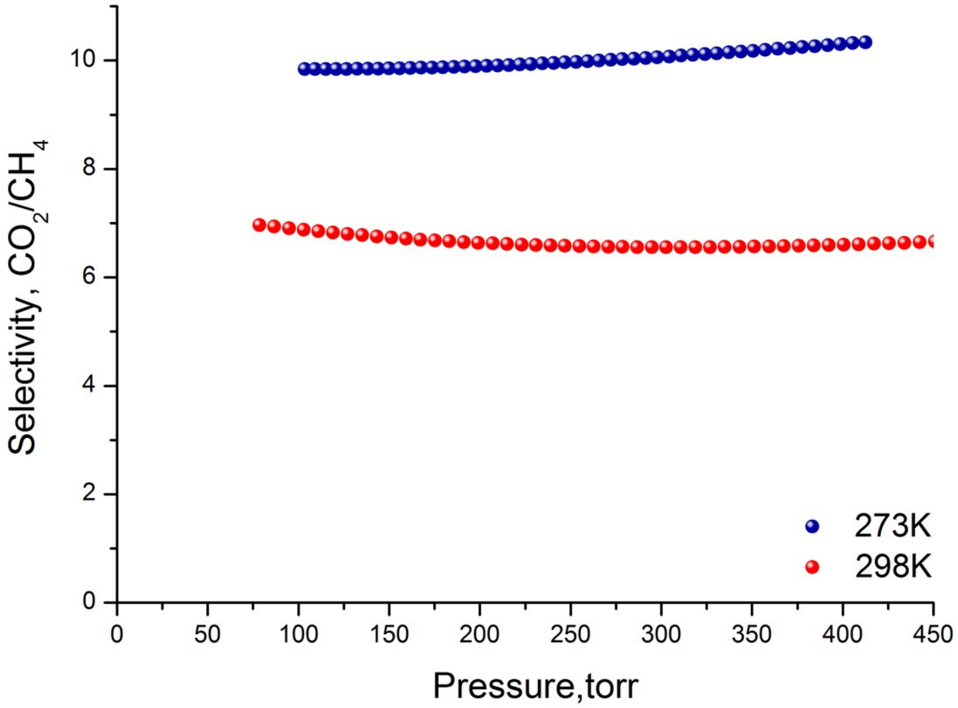

Figure S39: Selectivities of CO_2 over CH_4 at 298 K and 273 K for **UCY-14** as predicted by IAST for a 5/95 CO_2/CH_4 molar mixture.

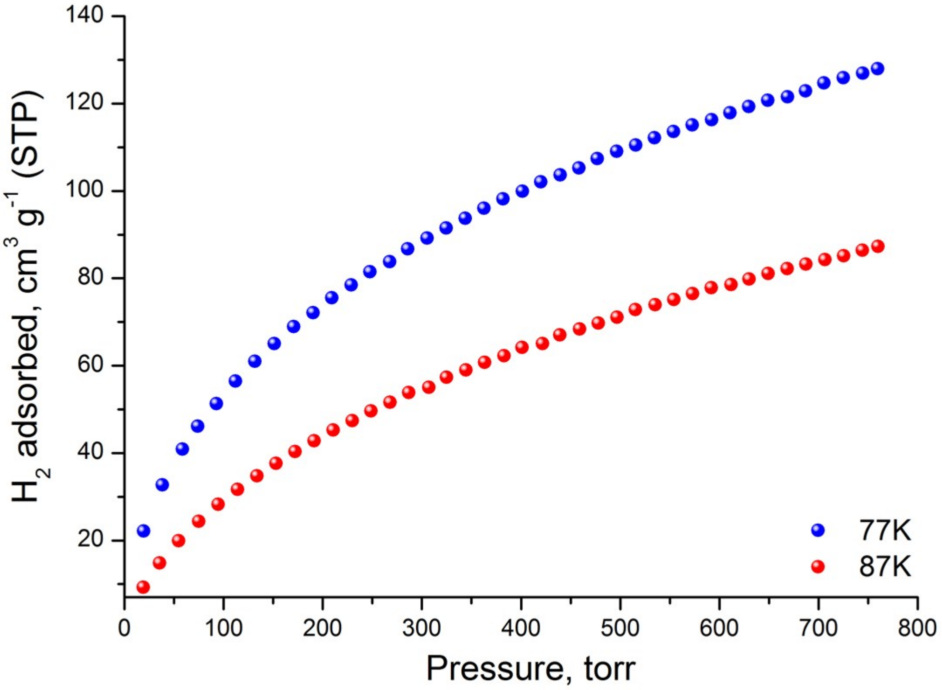

Figure S40: H_2 adsorption isotherms of **UCY-13** at 77 K and 88 K.

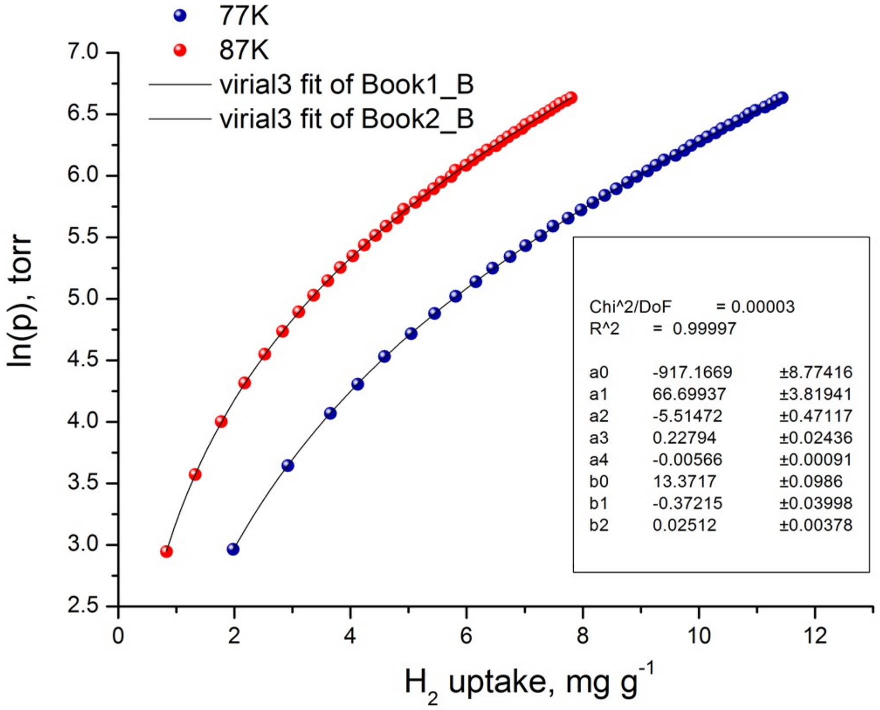

Figure S41: Virial type fitting of H_2 adsoprtion isotherms of **UCY-13** at 77 K and 88 K according to equation 1.

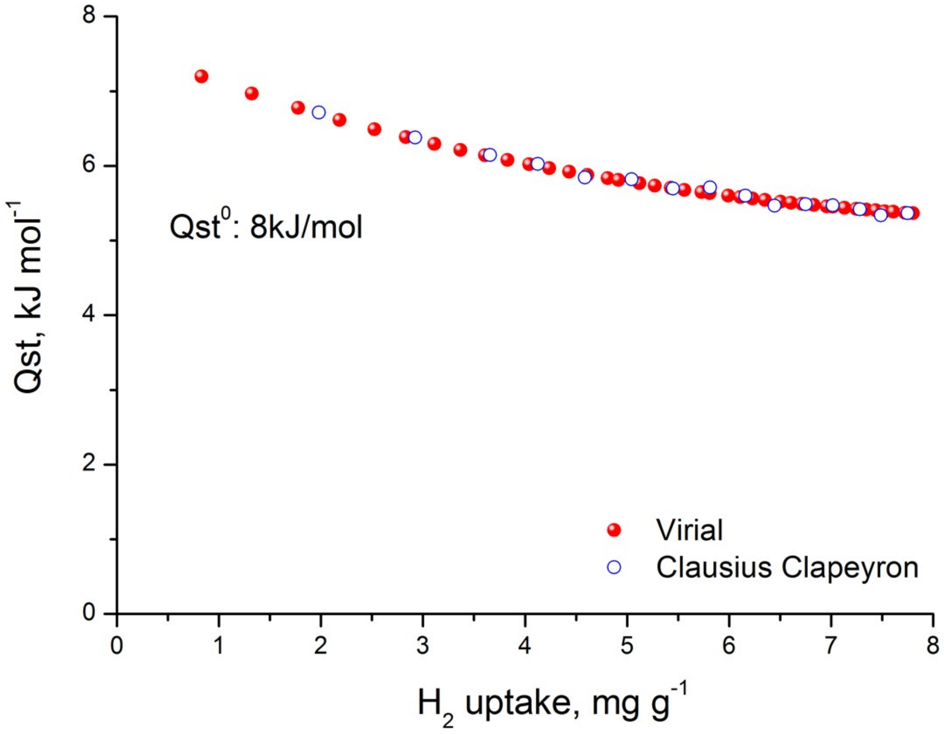

Figure S42: H_2 isosteric heat of adsorption in **UCY-13** as a function of surface coverage.

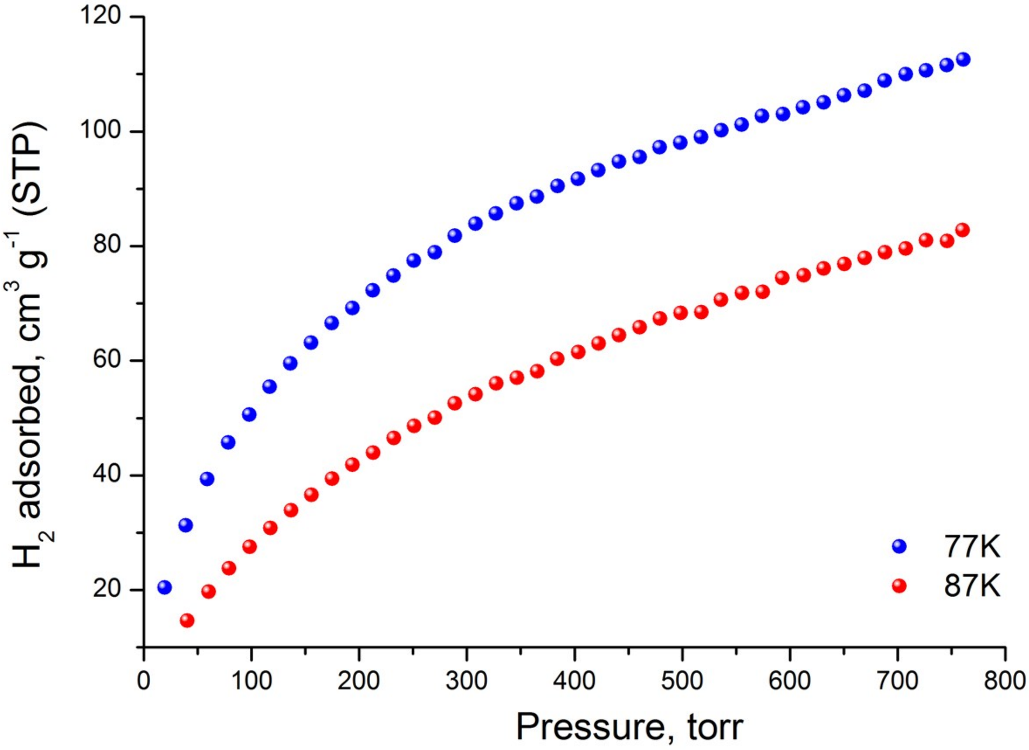

Figure S43: H_2 adsorption isotherms of **UCY-14** at 77 K and 88 K.

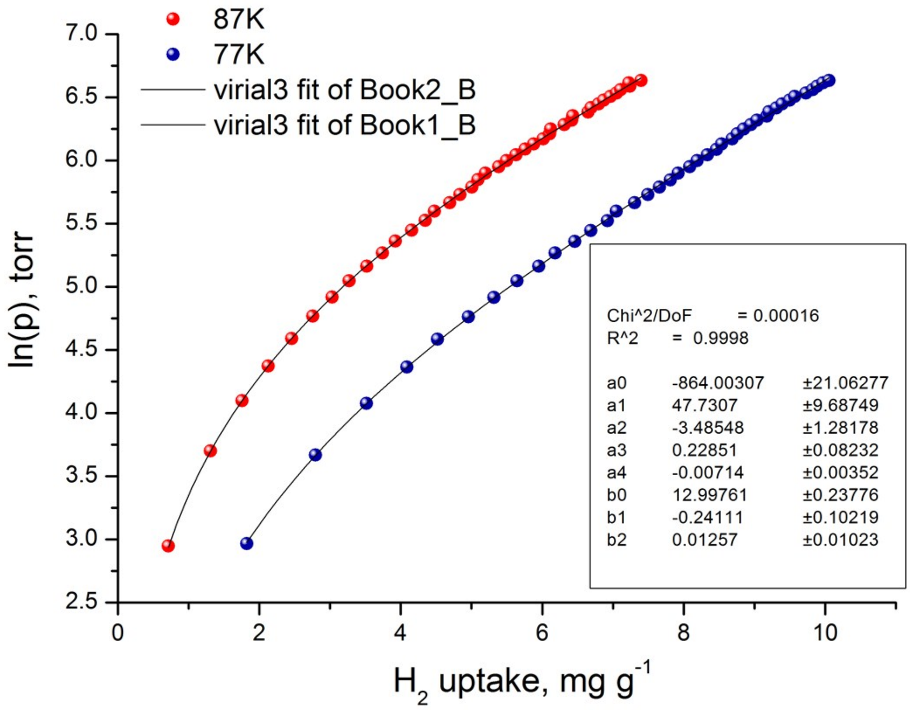

Figure S44: Virial type fitting of H_2 adsorption isotherms of **UCY-14** at 77 K and 88 K according to equation 1.

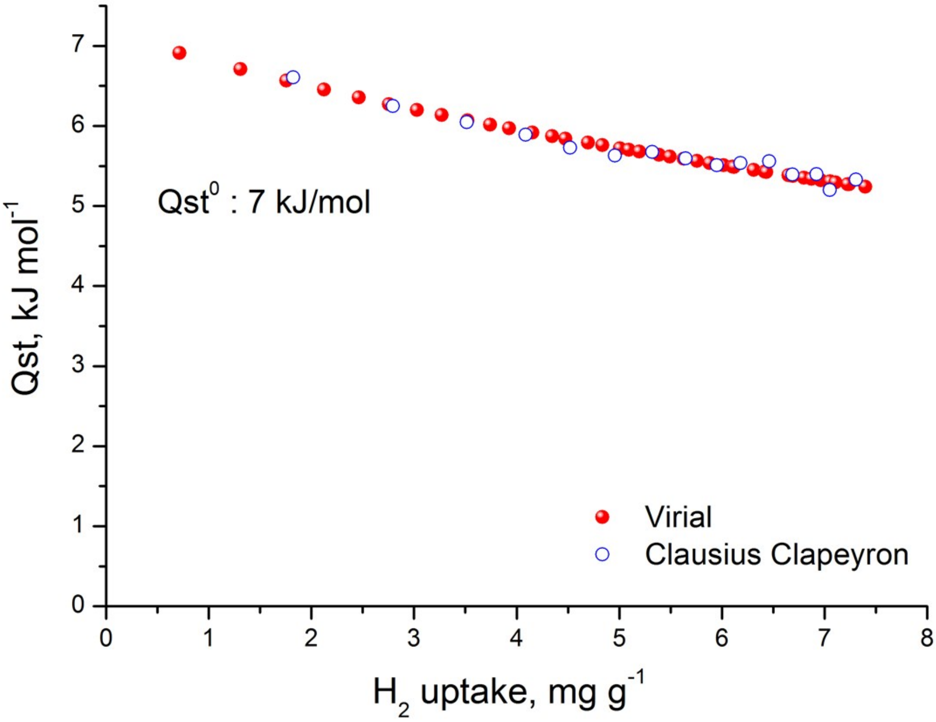

Figure S45: H_2 isosteric heat of adsorption in **UCY-14** as a function of surface coverage.

Uranyl Sorption Measurements

MOF/MOF based material	Adsorption Capacity (mg/g)	pH	Equilibrium Time (mins)	Reusability	Mechanism	Ref.
UiO-66	109.9	5.5	300	Not Reported	I.E. [b]	[16]
UiO-66-NH_2	114.9	5.5	300	Not Reported	I.E. [b]	[16]
UiO-66AO	2.68(seawater)	~7.8	120	Reusable	C.L.F.G.[c]	[17]
UiO-68-P(O)$(OEt)_2$	217	2.5	60	Not fully desorbed	C.L.F.G. [c]	[18]
	152	5	60			
UiO-68-P(O)$(OH)_2$	109	2.5	60	Not fully desorbed	C.L.F.G.[c]	[18]
	104	5	60			
GO-COOH/UiO-66	188.3	8	230	Reusable	I.E. [b]	[19]
HKUST-1	787.4	6	60	Low desorption yield	E.I. [d]	[20]
MIL-101	20	5.5	120	Not Reported	N/A	[21]
MIL-101-NH_2	90	5.5	120	Reusable	CLFG [c]	[21]
MIL-101-ED	200	5.5	120	Reusable[a]	CLFG [c]	[21]
MIL-101-DETA	350	5.5	120	Reusable[a]	CLFG [c]	[21]
MOF-76	298	3	60	Reusable	I.E. [b]	[22]
UCY-13	984	3	120	Not Desorbed	C.D.SBU [e]	this work
UCY-14	471	3	120	Not Desorbed	C.D.SBU [e]	this work

Table S2: Uranyl sorption by representative MOFs.

[a] A small decrease (~ 30 %) of the UO_2^{2+}sorption capacity of the re-used material was observed. [b] I.E.: Ion Exchange; [c] C.L.F.G.: Coordination to ligand's functional groups; [d] E.I.: Electrostatic Interactions, [e] C.D.SBU: Coordination to donor groups of the SBU

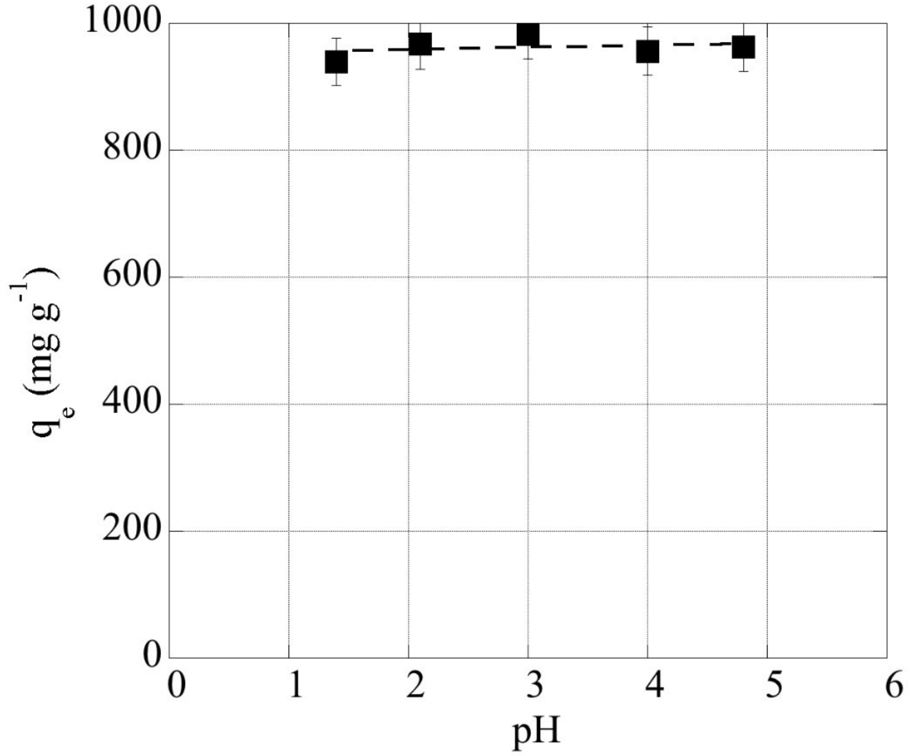

Figure S46: Effect of pH on U(VI) sorption by **UCY-13**, C_{in} = 0.5mM, pH = 1 - 5 ± 0.1, I = 0.1M ($NaClO_4$), $m_{sorbent}$: **UCY-13** = 0.033g, $V_{solution}$ = 30 ml and T = 296 ± 2 K.

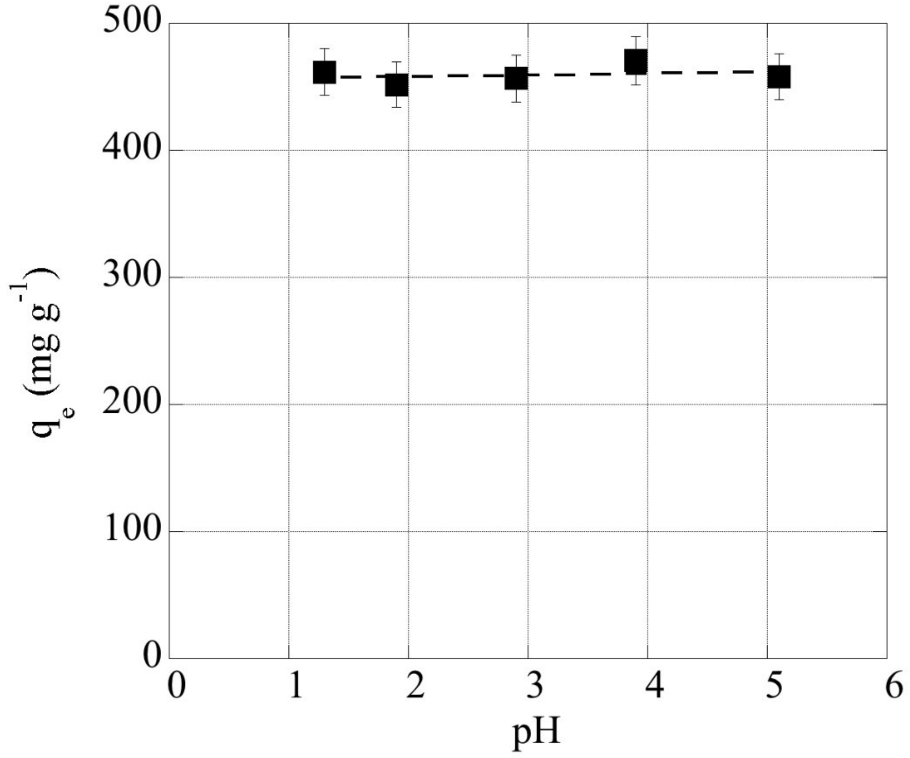

Figure S47: Effect of pH on U(VI) sorption by **UCY-14**, C_{in} = 0.5mM, pH = 1 - 5 ± 0.1, I = 0.1M ($NaClO_4$), $m_{sorbent}$: **UCY-14** = 0.033g, $V_{solution}$ = 30 ml and T = 296 ± 2 K.

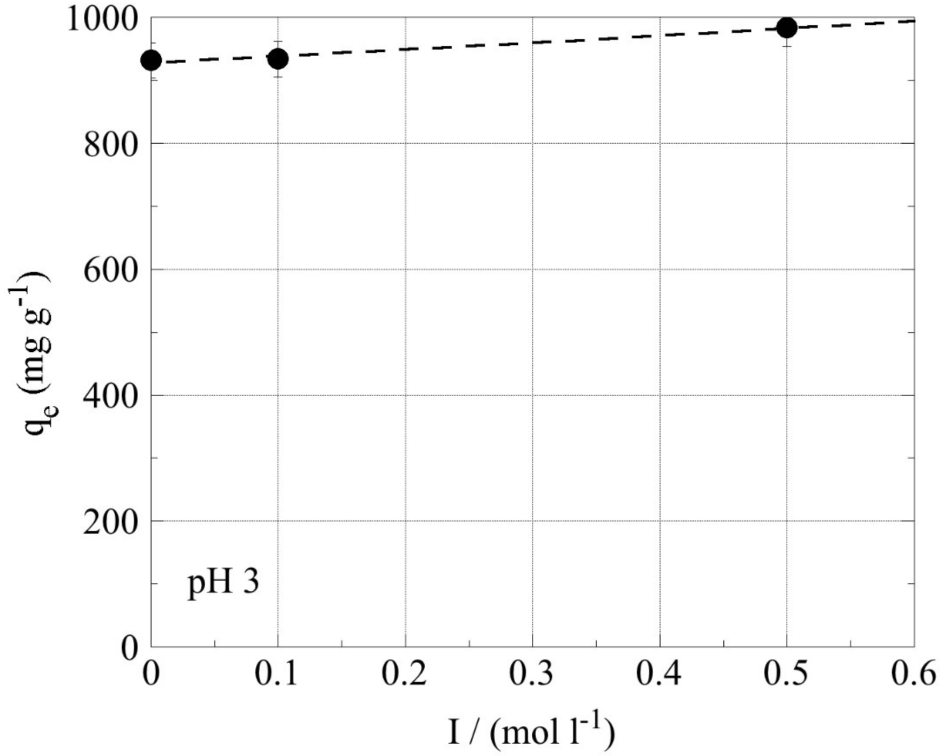

Figure S48: Effect of ionic strength on U(VI) sorption by **UCY-13**, C_{in} = 0.5mM, pH = 3 ± 0.1, I = 0 – 0.5M ($NaClO_4$), $m_{sorbent}$: **UCY-13** = 0.033g, $V_{solution}$ = 30 ml and T = 296 ± 2 K.

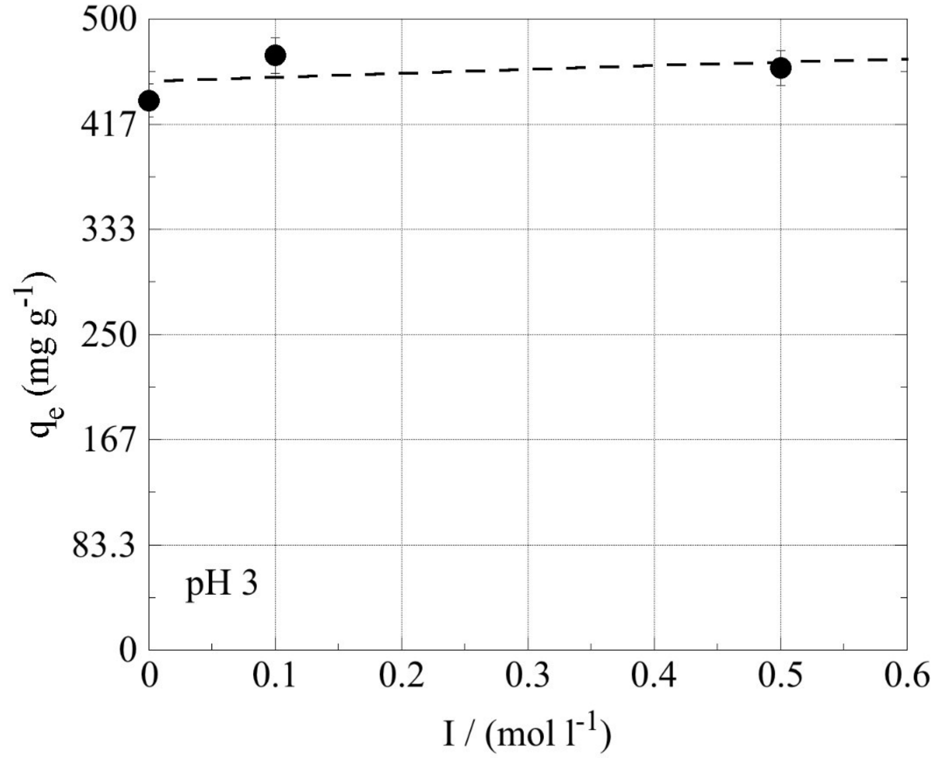

Figure S49: Effect of ionic strength on U(VI) sorption by **UCY-14**, C_{in} = 0.5mM, pH = 3 ± 0.1, I = 0 – 0.5M ($NaClO_4$), $m_{sorbent}$: **UCY-14** = 0.033g, $V_{solution}$ = 30 ml and T = 296 ± 2 K.

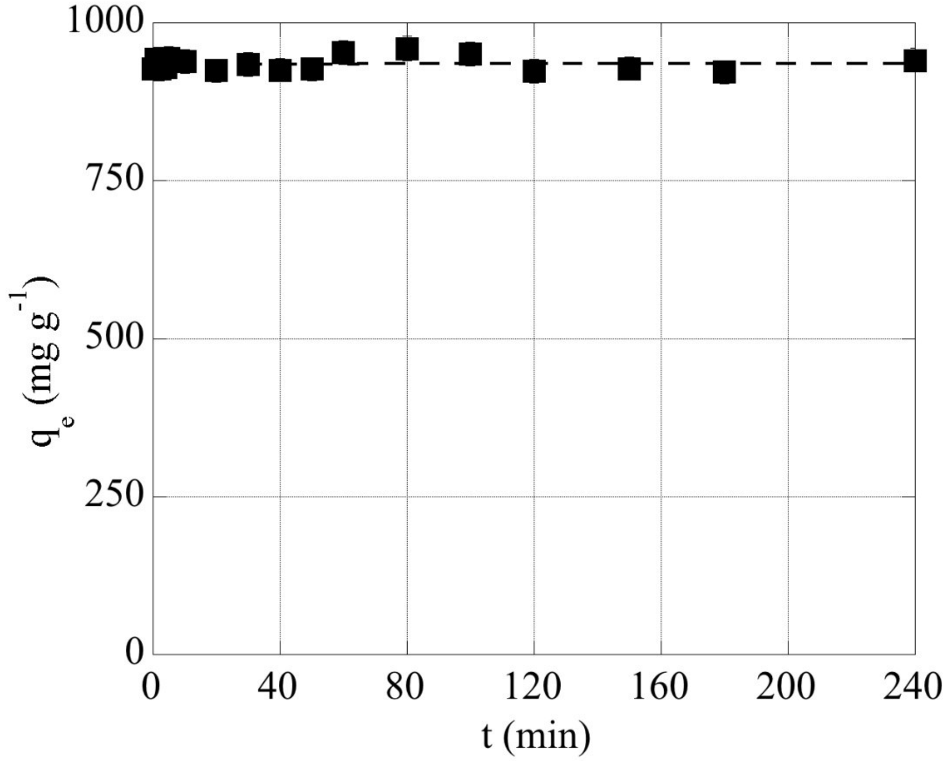

Figure S50: The kinetics of U(VI) sorption by **UCY-13**, C_{in} = 0.5mM, pH = 3 ± 0.1, I = 0.1M ($NaClO_4$), $m_{sorbent}$: **UCY-13** = 0.033g, $V_{solution}$ = 100 ml and T = 296 ± 2 K.

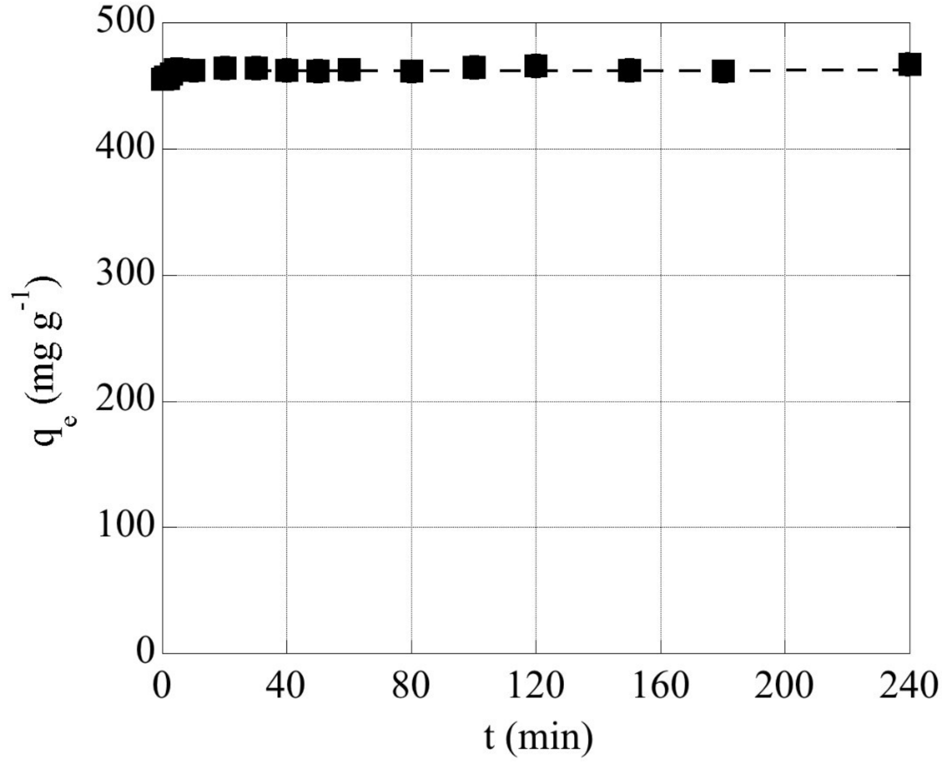

Figure S51: The kinetics of U(VI) sorption by **UCY-14**, C_{in} = 0.5mM, pH = 3 ± 0.1, I = 0.1M ($NaClO_4$), **UCY-14** = 0.033g, $V_{solution}$ = 100 ml and T = 296 ± 2 K.

Characterization of U(VI)@MOF Materials

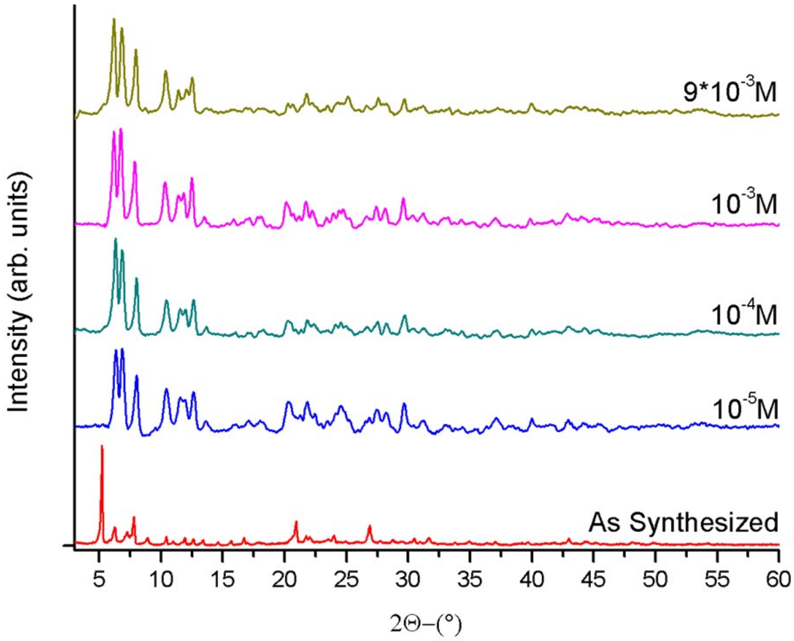

Figure S52: Powder X-ray diffraction patterns of U(VI)@**UCY-13** (**UCY-13** containing U(VI) into its pores); C_{in} = shown in the figure, pH 3 ± 0.1, I = 0.1M ($NaClO_4$), t = 120 min, $m_{sorbent}$: **UCY-13** = 0.033g, $V_{solution}$ = 30 ml and T = 296 ± 2 K.

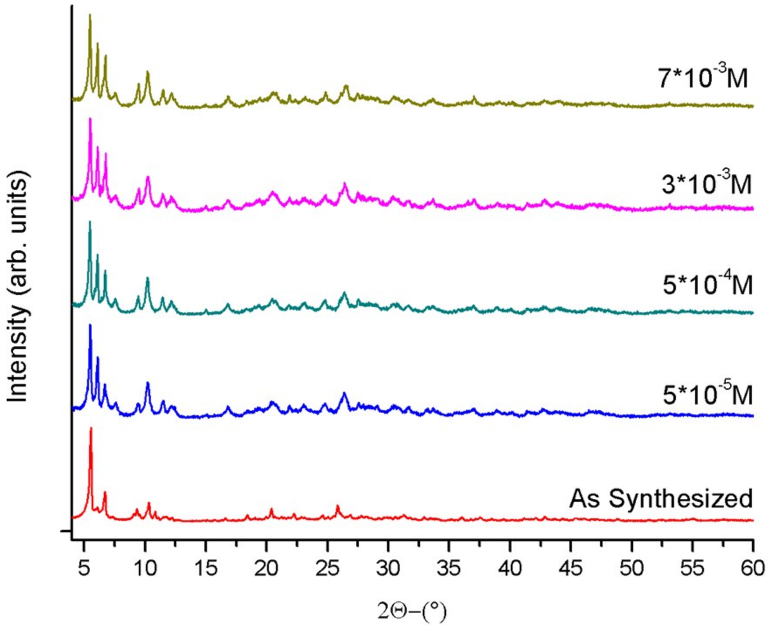

Figure S53: Powder X-ray diffraction patterns of U(VI)@**UCY-14** (**UCY-14** containing U(VI) into its pores); C_{in} = shown in the figure, pH 3 ± 0.1, I = 0.1M ($NaClO_4$), t = 120 min, $m_{sorbent}$: **UCY-14** = 0.033g, $V_{solution}$ = 30 ml and T = 296 ± 2 K. Blank: 0.1M $NaClO_4$ and $NaNO_3$ 0.5mM.

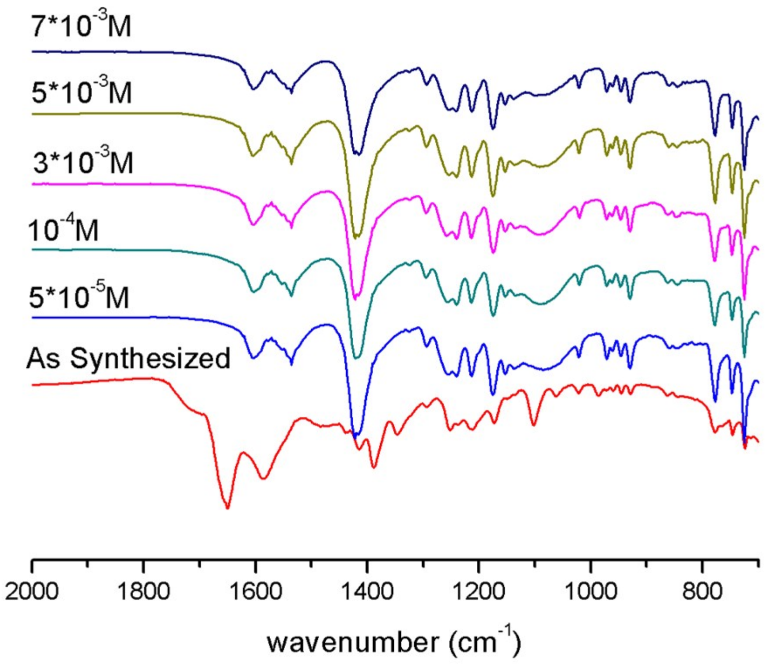

Figure S54: IR spectra of U(VI)@**UCY-13** (**UCY-13** containing U(VI) into its pores); C_{in} = shown in the figure, pH 3 ± 0.1, I = 0.1M ($NaClO_4$), t = 120 min, $m_{sorbent}$: **UCY-13** = 0.033g, $V_{solution}$ = 30 ml and T = 296 ± 2 K.

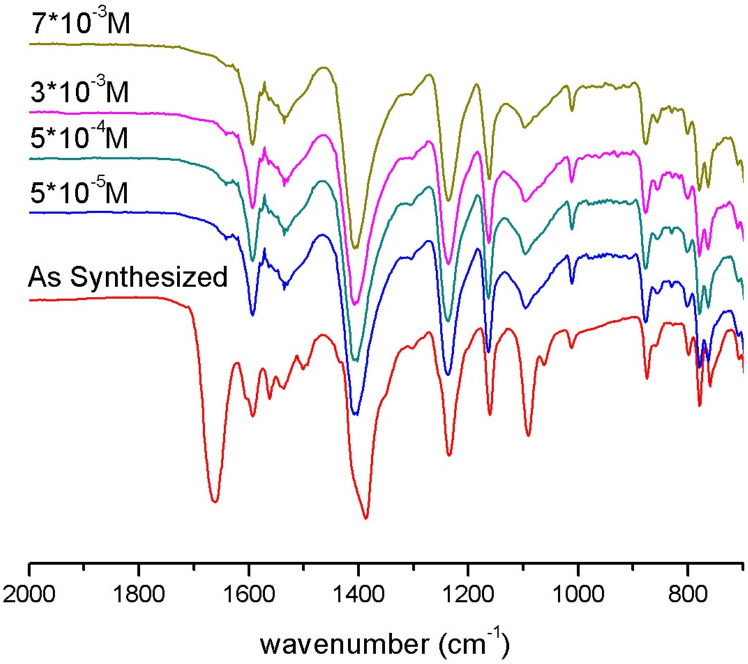

Figure S55: IR spectra of U(VI)@**UCY-14** (**UCY-14** containing U(VI) into its pores); C_{in} = shown in the figure, pH 3 ± 0.1, I = 0.1M ($NaClO_4$), t = 120 min, $m_{sorbent}$: **UCY-14** = 0.033g, $V_{solution}$ = 30 ml and T = 296 ± 2 K.

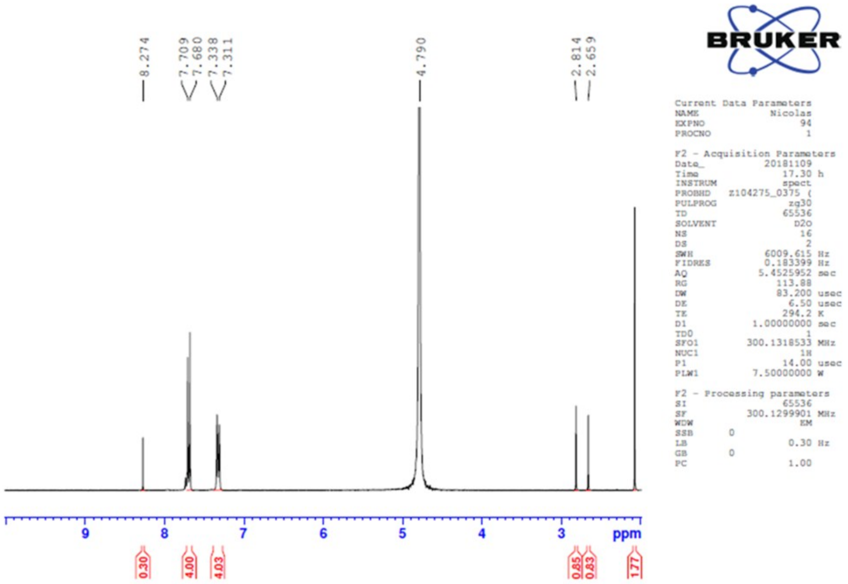

```
Current Data Parameters
NAME              Nicolas
EXPNO                  94
PROCNO                  1

F2 - Acquisition Parameters
Date_            20181109
Time              17.30 h
INSTRUM             spect
PROBHD     Z104275_0375 (
PULPROG              zg30
TD                  65536
SOLVENT               D2O
NS                     16
DS                      2
SWH              6009.615 Hz
FIDRES           0.183399 Hz
AQ              5.4525952 sec
RG                 113.88
DW                 83.200 usec
DE                   6.50 usec
TE                  294.2 K
D1             1.00000000 sec
TD0                     1
SFO1          300.1318533 MHz
NUC1                   1H
P1                  14.00 usec
PLW1           7.50000000 W

F2 - Processing parameters
SI                  65536
SF            300.1299901 MHz
WDW                    EM
SSB        0
LB                   0.30 Hz
GB         0
PC                   1.00
```

Figure S56: ^{1}H-NMR spectrum of treated **UCY-13** (magnetic stirring for 2 hours of 33 mg of **UCY-13** in a solution containing $NaClO_4$ 0.1M with pH = 3) digested in 0.5M KOH in D_2O. This measurement indicates that no ligand decomposition takes place at the corresponding conditions since no additional peaks appear compared to the ^{1}H NMR spectrum of as synthesized **UCY-13** shown in fig S15 (for peaks assignment see the caption of fig S15).

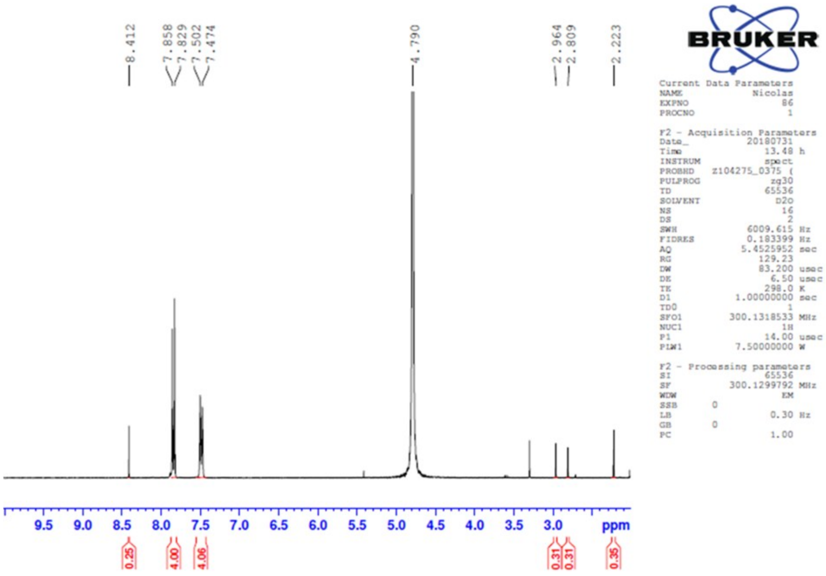

Figure S57: ^{1}H-NMR spectrum of U(VI)@**UCY-13** (**UCY-13** containing U(VI) into its pores); $C_{in}(UO_2(NO_3)_2)$ = 1mM, pH 3 ± 0.1, I = 0.1M ($NaClO_4$), t = 120 min, $m_{sorbent}$: **UCY-13** = 0.033g, $V_{solution}$ = 30 ml and T = 296 ± 2 K) digested in 0.5M KOH in D_2O. This measurement indicates that no ligand decomposition takes place at the corresponding conditions since no additional peaks appear in this spectrum compared to the ^{1}H NMR spectrum of as synthesized **UCY-13** shown in fig S15 (for the assignment of the peaks see the caption of figS15).

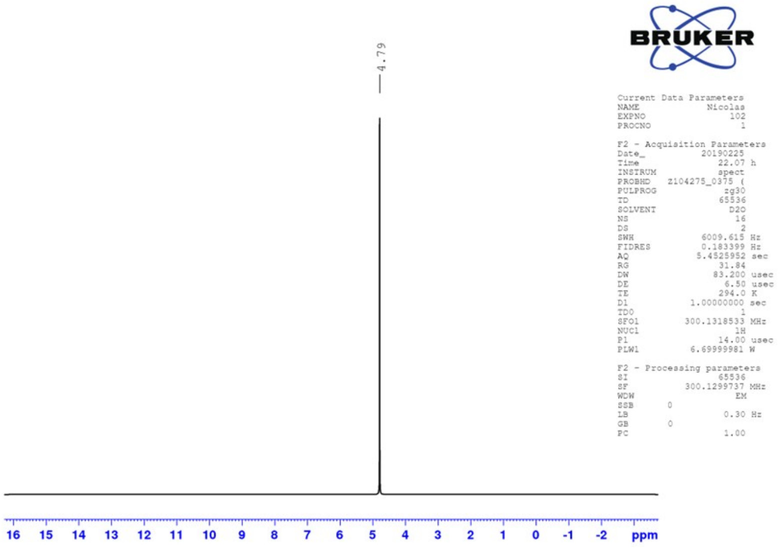

Figure S58: ^{1}H-NMR spectrum of the supernatant liquid after U(VI) sorption into the framework of **UCY-13**; $C_{in}(UO_2(NO_3)_2)$ = 1mM, pH 3 ± 0.1, I = 0.1M ($NaClO_4$), t = 120 min, $m_{sorbent}$: **UCY-13** = 0.033g, $V_{solution}$ = 30 ml and T = 296 ± 2 K. This measurement indicates that no ligand leaching and MOF decomposition takes place upon U(VI) sorption into the framework of **UCY-13** since the only peak appearing in the spectrum (δ 4.790) is assigned to H_2O H atoms.

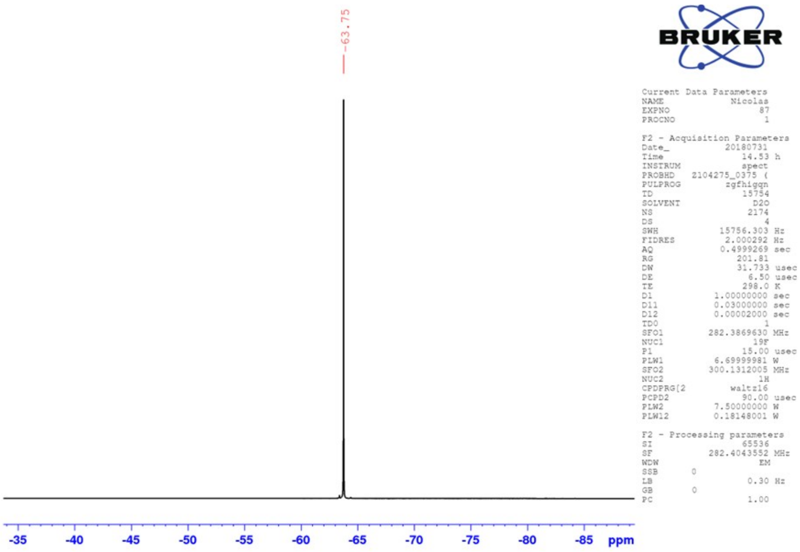

Figure S59: ^{19}F-NMR spectrum of U(VI)@**UCY-13** (**UCY-13** containing U(VI) into its pores) digested in 0.5M KOH in D_2O; $C_{in}(UO_2(NO_3)_2)$ = 1mM, pH 3 ± 0.1, I = 0.1M ($NaClO_4$), t = 120 min, $m_{sorbent}$: **UCY-13** = 0.033g, $V_{solution}$ = 30 ml and T = 296 ± 2 K. This measurement indicates that no ligand decomposition takes place at the corresponding conditions since there is only one peak appearing at this spectrum (δ -63.75) as happens in the ^{19}F-NMR spectrum of as synthesized **UCY-13** digested in 0.5M KOH in D_2O shown in fig S16.

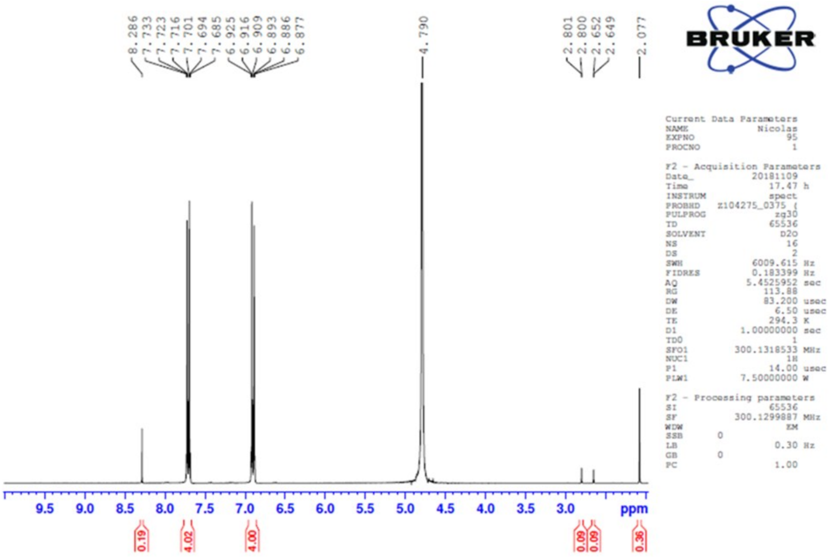

Figure S60: ^{1}H-NMR spectrum of treated **UCY-14** (magnetic stirring for 2 hours of 33 mg of **UCY-14** in a solution containing $NaClO_4$ 0.1M with pH = 3) digested in 0.5M KOH in D_2O. This measurement indicates that no ligand decomposition takes place at the corresponding conditions since no additional peaks appear in this spectrum compared to the ^{1}H NMR spectrum of as synthesized **UCY-14** shown in fig S19 (for the assignment of the peaks see the caption of figS19). This measurement also indicates the partial removal of lattice DMF and formic acid molecules and ligated formate during this treatment.

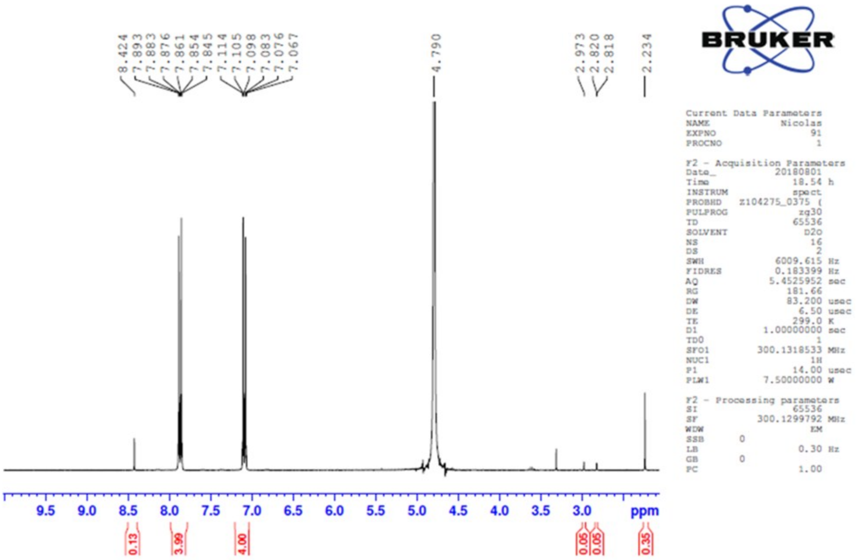

Figure S61: ^{1}H-NMR spectrum of U(VI)@**UCY-14** (**UCY-14** containing U(VI) into its pores) digested in 0.5M KOH in D_2O; $C_{in}(UO_2(NO_3)_2)$ = 9mM, pH 3 ± 0.1, I = 0.1M ($NaClO_4$), t = 120 min, $m_{sorbent}$: **UCY-14** = 0.033g, $V_{solution}$ = 30 ml and T = 296 ± 2 K. This measurement indicates that no ligand decomposition takes place at the corresponding conditions since no additional peaks appear in this spectrum compared to the ^{1}H NMR spectrum of as synthesized **UCY-14** shown in fig S19 (for the assignment of the peaks see the caption of fig S19).

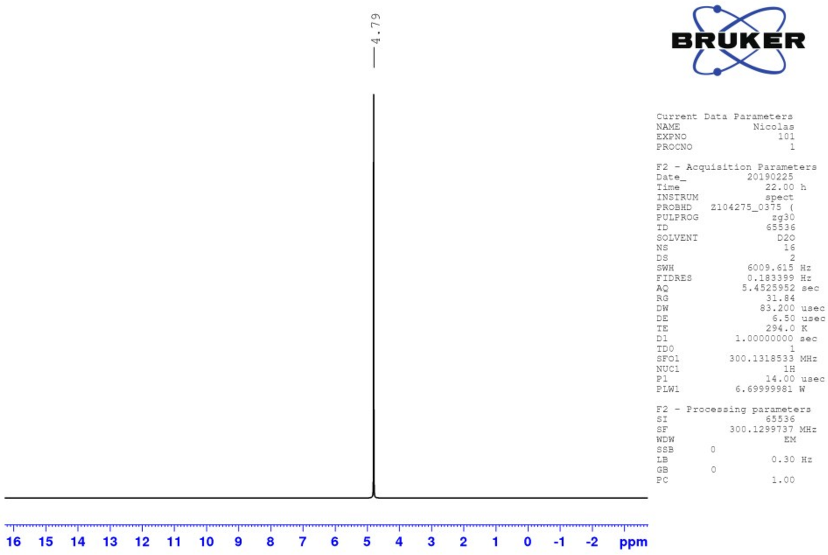

Figure S62: ^{1}H-NMR spectrum of the supernatant liquid after U(VI) sorption by **UCY-14**; $C_{in}(UO_2(NO_3)_2)$ = 9mM, pH 3 ± 0.1, I = 0.1M ($NaClO_4$), t = 120 min, $m_{sorbent}$: **UCY-14** = 0.033g, $V_{solution}$ = 30 ml and T = 296 ± 2 K. This measurement indicates that no ligand leaching and MOF decomposition takes place upon U(VI) sorption into the framework of **UCY-14** since the only peak appearing in the spectrum ($\delta = 4.790$ ppm) is assigned to H_2O H atoms.

$$\{H_{16}[Zr_6O_{16}(HFPBBA)_4]\}_n + 10nUO_2(NO_3)_2 + 10ynH_2O \longrightarrow$$

$$\{H_{16-x}[Zr_6O_{16}(HFPBBA)_4((UO_2(H_2O)_y)_{10}(NO_3)_{20-x})]\}_n + xnH^+ + xnNO_3^- \qquad \textbf{\textit{Equation 1}}$$

$$\{H_{13}[Zr_6O_{14}(OBA)_4(HCOO)]\}_n + 4nUO_2(NO_3)_2 + (4y+2)nH_2O \longrightarrow$$

$$\{H_{16-x}[Zr_6O_{16}(OBA)_4((UO_2(H_2O)_y)_4(NO_3)_{8-x})]\}_n + xnH^+ + xnNO_3^- + nHCOOH \qquad \textbf{\textit{Equation 2}}$$

Scheme S1: Stoichiometric chemical equations representing UO_2^{2+} sorption by **UCY-13** (Equation 1) and **UCY-14** (Equation 2). Note that when **UCY-14** is exposed in aqueous solutions the ligated bridging $HCOO^-$ is replaced by terminal OH^- and H_2O molecules as indicated by ^{1}H NMR spectra of the digested in 0.5 M KOH material (see Fig. S60).

Table S3: Composition of the Commercial Mineral Water (CMW) used in this study.

Ion	Quantity (mg/L)
Ca^{2+}	93.1
Mg^{2+}	1.9
Na^{+}	2.6
K^{+}	0.1
NH_4^{+}	<0.1
HCO_3^{-}	270
Cl^{-}	9
SO_4^{2-}	12.2
NO_3^{-}	7.2
NO_2^{-}	<0.05

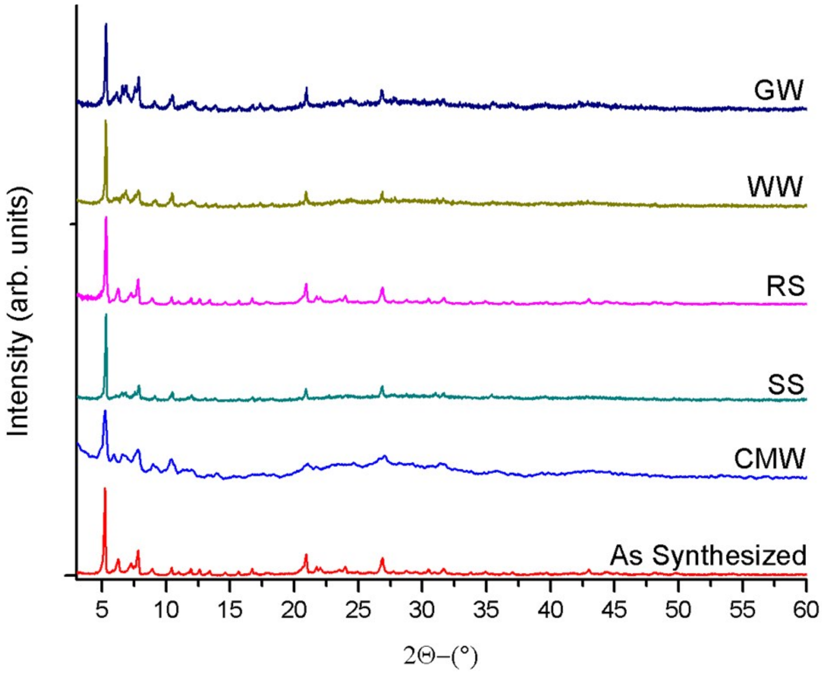

Figure S63: Powder X-ray diffraction patterns after stirring for 2 hours a suspension of **UCY-13**, in various aqueous media (CMW: commercial mineral water, SSW: simulated seawater, RSW: real seawater, WW: wastewater, GW: ground water); $m_{sorbent}$: **UCY-13** = 0.1g, $V_{solution}$ = 30 ml and T = 296 ± 2 K.

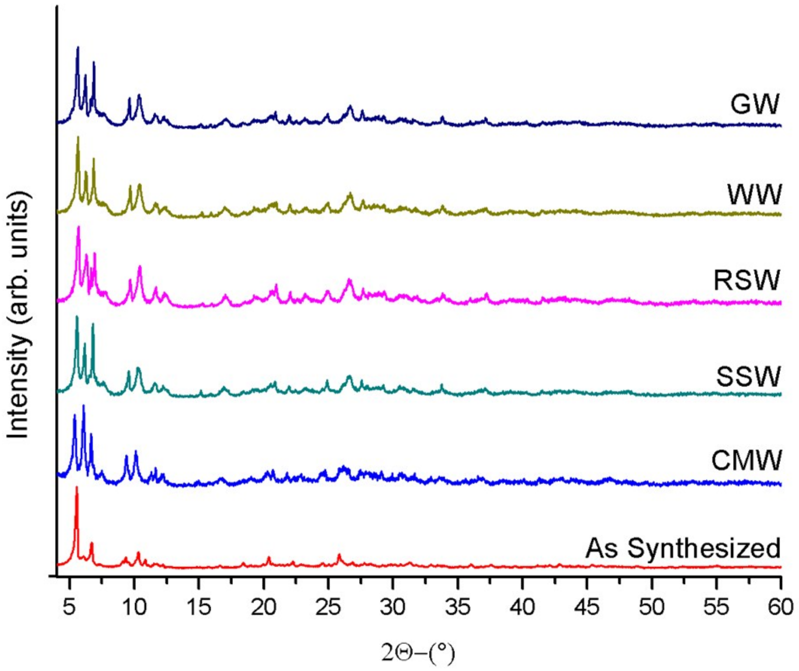

Figure S64: Powder X-ray diffraction patterns after stirring for 2 hours a suspension of **UCY-14**, in various aqueous media (CMW: commercial mineral water, SSW: simulated seawater, RSW: real seawater, WW: wastewater, GW: ground water); $m_{sorbent}$: **UCY-14** = 0.1g, $V_{solution}$ = 30 ml and T = 296 ± 2 K.

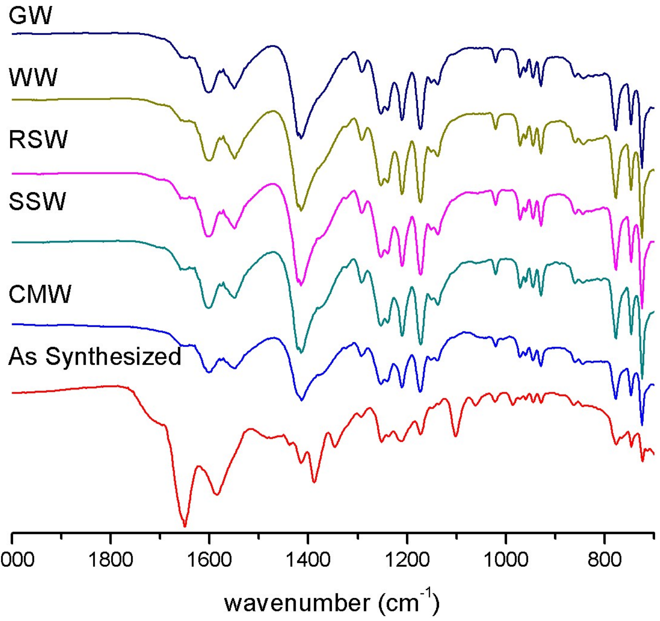

Figure S65: IR spectra of treated **UCY-13** (magnetic stirring for 2 hours of a suspension of **UCY-13**, in various aqueous media; CMW: commercial mineral water, SSW: simulated seawater, RSW: real seawater, WW: wastewater, GW: ground water); $m_{sorbent}$: **UCY-13** = 0.1g, $V_{solution}$ = 30 ml and T = 296 ± 2 K.

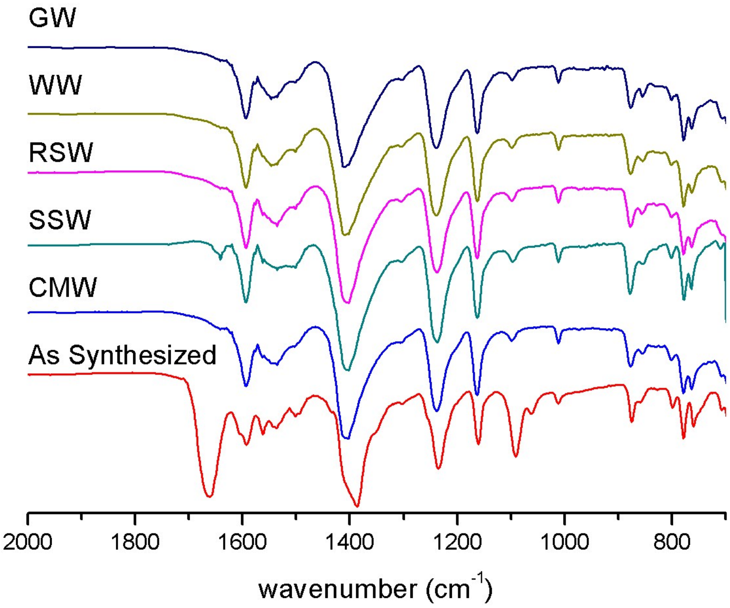

Figure S66: IR spectra of treated **UCY-14** (magnetic stirring for 2 hours of a suspension of **UCY-14**, in various aqueous media; CMW: commercial mineral water, SSW: simulated seawater, RSW: real seawater, WW: wastewater, GW: ground water); $m_{sorbent}$: **UCY-14** = 0.1g, $V_{solution}$ = 30 ml and T = 296 ± 2 K.

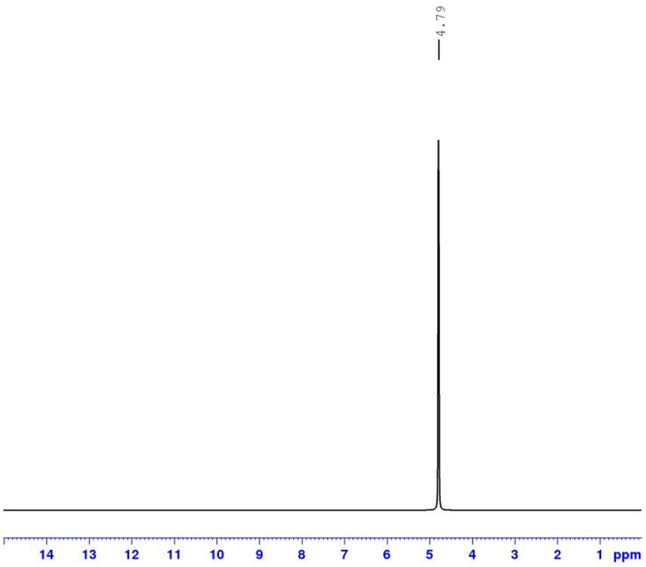

```
Current Data Parameters
NAME               Nicolas
EXPNO                   96
PROCNO                   1

F2 - Acquisition Parameters
Date_            20181218
Time                15.45 h
INSTRUM              spect
PROBHD   Z104275_0375 (
PULPROG               zg30
TD                   65536
SOLVENT                D2O
NS                      16
DS                       2
SWH               6009.615 Hz
FIDRES            0.183399 Hz
AQ               5.4525952 sec
RG                   24.55
DW                  83.200 usec
DE                    6.50 usec
TE                   294.1 K
D1              1.00000000 sec
TD0                      1
SFO1           300.1318533 MHz
NUC1                    1H
P1                   14.00 usec
PLW1            7.50000000 W

F2 - Processing parameters
SI                   65536
SF             300.1299763 MHz
WDW                     EM
SSB      0
LB                    0.30 Hz
GB       0
PC                    1.00
```

Figure S67: ^{1}H-NMR spectrum of the filtrate resulted from the treatment (magnetic stirring for 2 hours) of **UCY-13** with CMW; $m_{sorbent}$: **UCY-13** = 0.033g, $V_{solution}$ = 30 ml and T = 296 ± 2 K. This measurement indicates that no ligand leaching and MOF decomposition takes place upon treatment of **UCY-13** with CMW1 since the only peak appeared in this spectrum (δ 4.790) is assigned to H_2O H atoms.

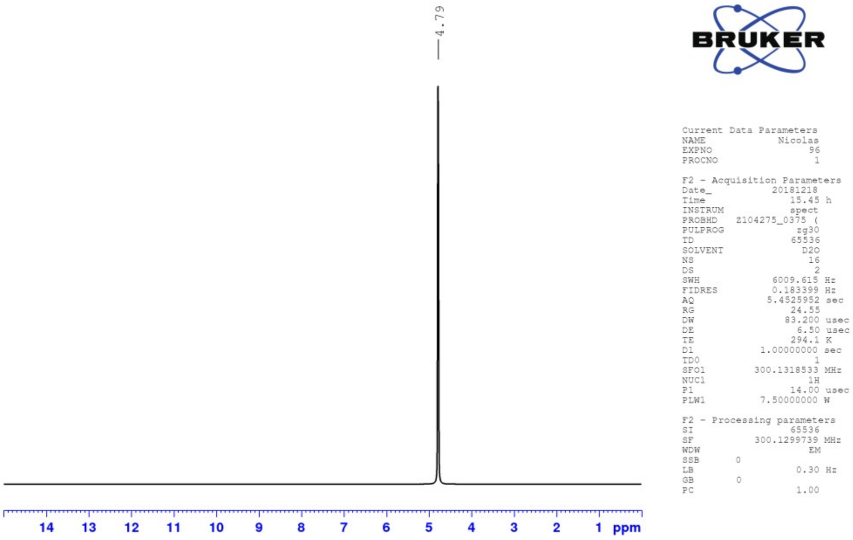

```
Current Data Parameters
NAME               Nicolas
EXPNO                   96
PROCNO                   1

F2 - Acquisition Parameters
Date_             20181218
Time                 15.45 h
INSTRUM              spect
PROBHD   Z104275_0375 (
PULPROG               zg30
TD                   65536
SOLVENT                D2O
NS                      16
DS                       2
SWH               6009.615 Hz
FIDRES            0.183399 Hz
AQ               5.4525952 sec
RG                   24.55
DW                  83.200 usec
DE                    6.50 usec
TE                   294.1 K
D1              1.00000000 sec
TD0                      1
SFO1           300.1318533 MHz
NUC1                    1H
P1                   14.00 usec
PLW1            7.50000000 W

F2 - Processing parameters
SI                   65536
SF             300.1299739 MHz
WDW                     EM
SSB      0
LB                    0.30 Hz
GB       0
PC                    1.00
```

Figure S68: ^{1}H-NMR spectrum of the filtrate resulted from the treatment (magnetic stirring for 2 hours) of **UCY-13**, in CMW in the presence of UO_2^{2+}(1ppm); $m_{sorbent}$: **UCY-13** = 0.033g, $V_{solution}$ = 30 ml and T = 296 ± 2 K. This measurement indicates that no ligand leaching, and MOF decomposition takes place upon U(VI) sorption by **UCY-13** in CMW1 since the only peak appeared in this spectrum (δ 4.790) is assigned to H_2O H atoms.

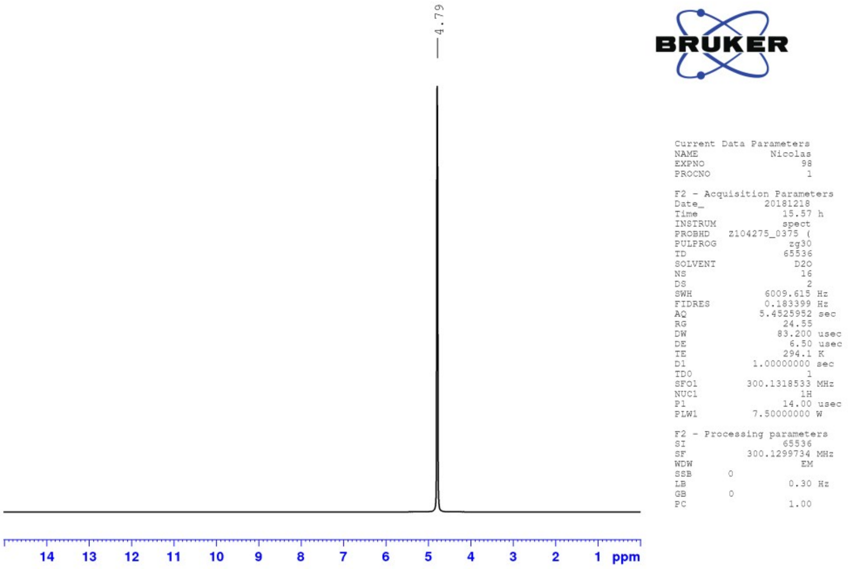

```
Current Data Parameters
NAME               Nicolas
EXPNO                   98
PROCNO                   1

F2 - Acquisition Parameters
Date_             20181218
Time                 15.57 h
INSTRUM              spect
PROBHD   Z104275_0375 (
PULPROG               zg30
TD                   65536
SOLVENT                D2O
NS                      16
DS                       2
SWH               6009.615 Hz
FIDRES            0.183399 Hz
AQ               5.4525952 sec
RG                   24.55
DW                  83.200 usec
DE                    6.50 usec
TE                   294.1 K
D1              1.00000000 sec
TD0                      1
SFO1           300.1318533 MHz
NUC1                    1H
P1                   14.00 usec
PLW1            7.50000000 W

F2 - Processing parameters
SI                   65536
SF             300.1299734 MHz
WDW                     EM
SSB      0
LB                    0.30 Hz
GB       0
PC                    1.00
```

Figure S69: ^{1}H-NMR spectrum of the filtrate resulted from the treatment (magnetic stirring for 2 hours) of **UCY-14** with CMW; $m_{sorbent}$: **UCY-14** = 0.033g, $V_{solution}$ = 30 ml and T = 296 ± 2 K. This measurement indicates that no ligand leaching and MOF decomposition takes place upon treatment of **UCY-14** with CMW1 since the only peak appeared in this spectrum (δ 4.790) is assigned to H_2O H atoms.

Figure S70: ^{1}H-NMR spectrum of the filtrate resulted from the treatment (magnetic stirring for 2 hours) of **UCY-14**, with CMW in the presence of UO_2^{2+}(1ppm); $m_{sorbent}$: **UCY-14** = 0.033g, $V_{solution}$ = 30 ml and T = 296 ± 2 K. This measurement indicates that no ligand leaching and MOF decomposition takes place upon U(VI) sorption by **UCY-14** in CMW1 since the only peak appeared in this spectrum (δ 4.790) is assigned to H_2O H atoms.

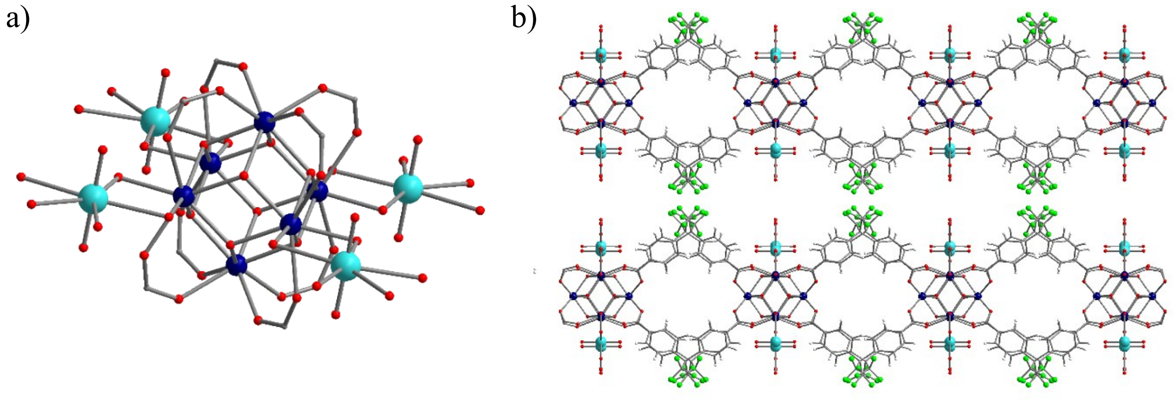

Figure S71: Representations of a) the $[Zr_6(\mu_3\text{-}O)_4(\mu_3\text{-}OH)_4(COO)_8(\mu_2\text{-}O)_4(\mu_2\text{-}OH)_4\{UO_2(H_2O)_3\}_4]$ SBU of a proposed U(VI)@**UCY-13** theoretical model created assuming that UO_2^{2+} ions are linked to the Zr_6 SBUs through their terminal OH/H_2O groups and b) the 2D framework of the U(VI)@**UCY-13** theoretical model along *a*-axis (uranium, turquoise; zirconium, dark blue; fluorine, light green; oxygen, red; carbon, grey; hydrogen, white).

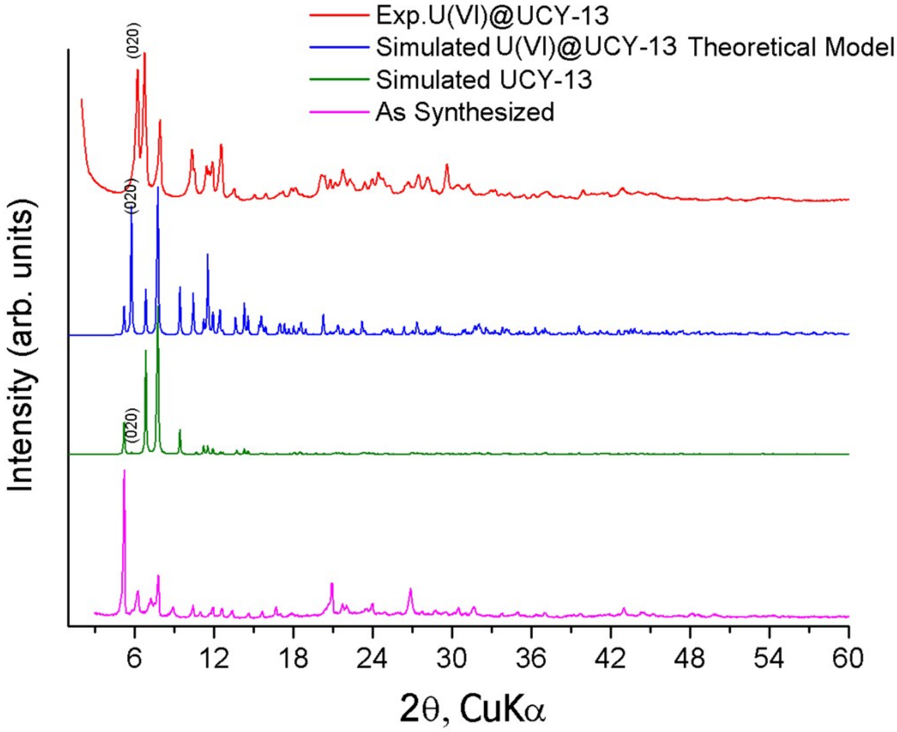

Figure S72: Simulated pxrd pattern produced from the proposed U(VI)@**UCY-13** theoretical model shown in figure S71 and its comparison with the indicated simulated/experimental pxrd patterns.

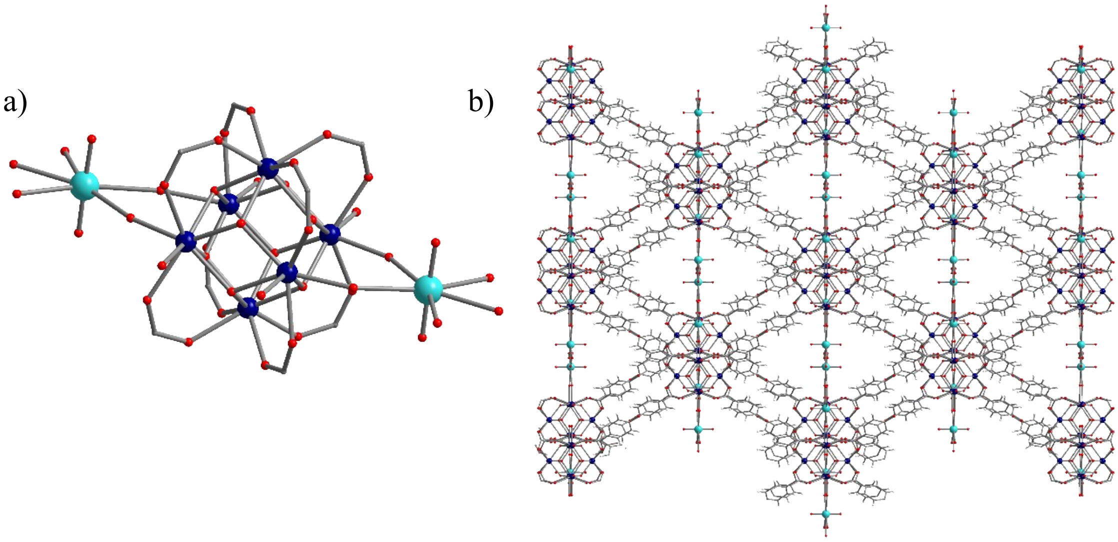

Figure S73: Representations of a) the $[Zr_6(\mu_3\text{-}O)_4(\mu_3\text{-}OH)_4(COO)_8(\mu_2\text{-}O)_2(\mu_2\text{-}$

OH)$_2${UO$_2$(H$_2$O)$_3$}$_2$(OH)$_2$(H$_2$O)$_2$] SBU of a proposed U(VI)@**UCY-14** theoretical model created assuming that UO_2^{2+} ions are linked to the Zr$_6$ SBUs through their terminal OH/H$_2$O groups and b) the 2D framework of the U(VI)@**UCY-14** theoretical model along *c*-axis (uranium, turquoise; zirconium, dark blue; oxygen, red; carbon, grey; hydrogen, white).

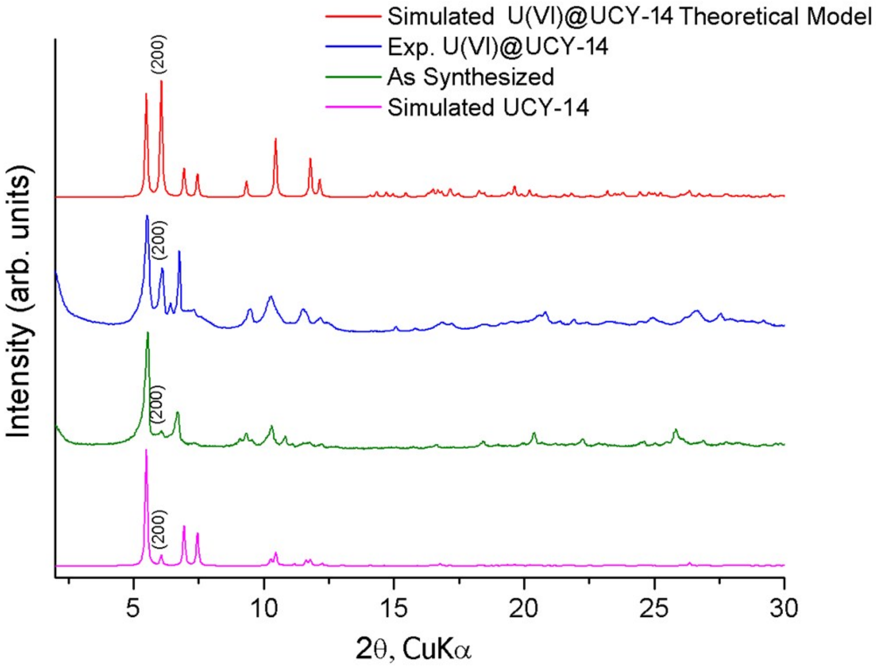

Figure S74: Simulated pxrd pattern produced from the proposed U(VI)@**UCY-14** theoretical model shown in figure S73 and its comparison with the indicated simulated/experimental pxrd patterns.

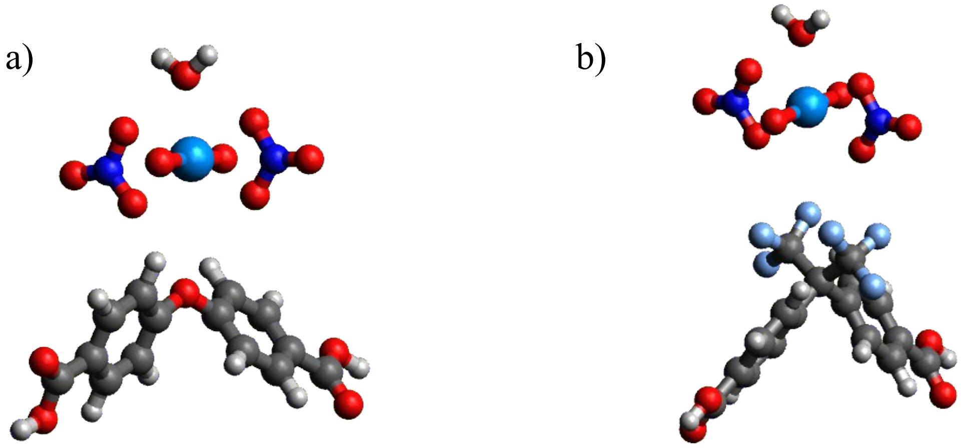

Figure S75: The optimized binding geometries of $UO_2(NO_3)_2(H_2O)$ complex with (a) H_2OBA and (b) $H_2HFPBBA$ linker. Uranium, carbon, oxygen, fluorine and hydrogen illustrated as blue, grey, red, light blue and white spheres, respectively.

References

1 K. Saito, T. Miyauchi, *J. Nucl. Sci. Technol.*, 1982, **19**, 145–150.

2 G. Sheldrick, *Acta Crystallogr. Sect. A*, 2008, **64**, 112–122.

3 Oxford Diffraction 2017, *CrysAlis CCD* and *CrysAlis RED*, version p171.38.46; Oxford Diffraction Ltd, Abingdon, Oxford, England.

4 L. J. Farrugia, *J. Appl. Crystallogr.*, 1999, **32**, 837–838.

5 K. Brandenburg, *DIAMOND* 2014, *Version 3.2k*, Crystal Impact GbR, Bonn,

Germany.

6 A. L. Spek, *J. Appl. Crystallogr.*, 2003, **36**, 7–13.

7 L. Hadjittofi, I. Pashalidis, *J. Radioanal. Nucl. Chem.*, 2015, **304**, 897–904.

8 M. H. Khan, P. Warwick, N. Evans, *Chemosphere*, 2006, **63**, 1165–1169.

9 T. Kiliari, I. Pashalidis, *Radiat. Meas.*, 2010, **45**, 966–968.

10 C. Charalambous, M. Aletrari, P. Piera, P. Nicolaidou-Kanari, M. Efstathiou, I. Pashalidis, *J. Environ. Radioact.*, 2013, **116**, 187–192.

11 L. Czepirski, J. JagieŁŁo, *Chem. Eng. Sci.*, 1989, **44**, 797–801.

12 K. Sumida, D. L. Rogow, J. A. Mason, T. M. McDonald, E. D. Bloch, Z. R. Herm, T.-H. Bae, J. R. Long, *Chem. Rev.*, 2012, **112**, 724–781.

13 A. L. Myers, J. M. Prausnitz, *AIChE J.*, 1965, **11**, 121–127.

14 Y.-S. Bae, K. L. Mulfort, H. Frost, P. Ryan, S. Punnathanam, L. J. Broadbelt, J. T. Hupp, R. Q. Snurr, *Langmuir*, 2008, **24**, 8592–8598.

15 G. S. Armatas, M. G. Kanatzidis, *Nat. Mater.*, 2009, **8**, 217–222.

16 B.-C. Luo, L.-Y. Yuan, Z.-F. Chai, W.-Q. Shi, Q. Tang, *J. Radioanal. Nucl. Chem.*, 2016, **307**, 269–276.

17 L. Chen, Z. Bai, L. Zhu, L. Zhang, Y. Cai, Y. Li, W. Liu, Y. Wang, L. Chen, J. Diwu, , J. Wang, Z. Chai, S. Wang, *ACS Appl. Mater. Interfaces*, 2017, **9**, 32446–32451.

18 M. Carboni, C. W. Abney, S. Liu, W. Lin, *Chem. Sci.*, 2013, **4**, 2396–2402.

19 P. Yang, Q. Liu, J. Liu, H. Zhang, Z. Li, R. Li, L. Liu, J. Wang, *J. Mater. Chem. A*, 2017, **5**, 17933–17942.

20 Y. Feng, H. Jiang, S. Li, J. Wang, X. Jing, Y. Wang, M. Chen, *Colloids Surfaces A Physicochem. Eng. Asp.*, 2013, **431**, 87–92.

21 Z.-Q. Bai, L.-Y. Yuan, L. Zhu, Z.-R. Liu, S.-Q. Chu, L.-R. Zheng, J. Zhang, Z.-F. Chai, W.-Q. Shi, *J. Mater. Chem. A*, 2015, **3**, 525–534.

22 W. Yang, Z.-Q. Bai, W.-Q. Shi, L.-Y. Yuan, T. Tian, Z.-F. Chai, H. Wang, Z.-M. Sun, *Chem. Commun.*, 2013, **49**, 10415–10417.